Marine Environmental Research 210 (2025) 107343

Contents lists available at ScienceDirect

Marine Environmental Research

journal homepage: www.elsevier.com/locate/marenvrev

Machine learning-based detection of changes in mapping the mangrove forest of the Yangon estuary, Southeast Asia

Phyu Phway Thant [a,c], Zhijun Dai [a,*], Xuefei Mei [a,b], Binh An Nguyen [d], Cong Mai Van [e], Mee Mee Soe [c]

[a] State Key Laboratory of Estuarine and Coastal Research, East China Normal University, Shanghai, China
[b] Ocean Decade International Cooperation Center, Qingdao, China
[c] Department of Port and Harbour Engineering, Myanmar Maritime University, Thanlyin, Yangon, Myanmar
[d] Ho Chi Minh City Institute of Resources Geography, Vietnam Academy of Science and Technology, Ho Chi Minh City, Viet Nam
[e] Faculty of Civil Engineering, Thuyloi University, Hanoi, Viet Nam

ARTICLE INFO

Keywords:
Mangrove forest
Eco-morphodynamics
Estuary
Yangon river
Machine learning

ABSTRACT

Mangrove forests are globally acknowledged for stabilizing coastlines, reducing wave energy, and protecting coastal habitats and adjacent land uses from extreme events. However, most regions experience alarming mangrove loss against natural and human disturbances. This study profiles dynamic changes in mangrove cover and shoreline migration along the Yangon estuary using Landsat imagery and machine learning approach from 1988 to 2023. Mangrove cover declined from 1175 ha in 1988 to 531 ha by 2011. It then increased to 5470 ha by 2023, resulting in a net gain of over 4000 ha. Concurrently, shoreline analysis using the mangrove vegetation line, indicates 92 % seaward progradation along the coastline. The western shoreline recorded mean accretion and erosion rates of +35.6 m/yr and −1.7 m/yr, while the eastern side showed more dynamic rates of +79.6 m/yr for accretion and −29.1 m/yr for erosion. Key findings highlight mangroves' ability to keep pace with the relative SLR, aquaculture as the dominant driver of post-2008 mangrove loss, and underscore the roles of sedimentary variation and high sediment availability, extensive tidal flat existence, and coastal sheltering in supporting recent mangrove expansion. While further studies are needed, these insights offer a valuable foundation for future conservation and management efforts.

1. Introduction

Located in tropical and subtropical intertidal regions, mangrove forests are among the world's richest ecosystems, supporting to land-building through sediment trapping, providing vital services such as flood regulation, shoreline protection, sediment trapping, biodiversity support, carbon sequestration, and climate adaptation (Anthony, 2004; Kumara et al., 2010; Brander et al., 2012; Alongi, 2016; Ahmed et al., 2018; Hamilton, 2019). Recognized as a key nature-based approach for climate resilience and disaster risk management (Sunkur et al., 2023), mangroves remain one of the most threatened tropical biomes (Field et al., 1998; Polidoro et al., 2010). According to the 2024 IUCN Red List of Mangrove Ecosystems, 50 % of mangrove units are at risk of collapse.

Global mangroves are largely found in Asia-Pacific, followed by the Americas and Africa (UNEP, 2023; Bunting et al., 2018, 2022). Between 2000 and 2020, approximately 284,000 ha of mangroves disappeared due to human and environmental stresses (FAO, 2023). Major anthropogenic factors include illegal logging, agricultural and aquaculture expansion, and urbanization (Richards and Friess, 2016; Ai et al., 2020; Leal and Spalding, 2022; Tinh et al., 2022). Natural factors such as hydrological and climatic changes also are having an impact on mangrove dynamics (Gilman et al., 2008; Alongi, 2009; Twilley and Day, 2013), with dominant drivers varied by region. Natural causes, for example, dominate in South America and Oceania, whereas human-caused impacts prevail in Asia and Africa (FAO, 2023).

Sea level rise (SLR) poses a major threat to mangroves (Gilman et al., 2008), as their survival depends on available accommodation space and species' ability to colonize new areas; while landward transgression may occur where space and adaptation allow, seaward mangroves risk drowning if they cannot keep pace with rising waters (Alongi, 2008). Mangrove response to SLR is complex. While mangroves in the Indo-Pacific struggle to keep pace with SLR (Lovelock et al., 2015), some

* Corresponding author.
E-mail address: zjdai@sklec.ecnu.edu.cn (Z. Dai).

https://doi.org/10.1016/j.marenvres.2025.107343
Received 6 April 2025; Received in revised form 1 July 2025; Accepted 2 July 2025
Available online 4 July 2025

coasts exhibit progradation (Long et al., 2021; Xiong et al., 2024). Mangrove range shifts are impeded by cold sensitivity, rainfall regimes, and salinity extremes, which affect species distribution differently across regions (Osland et al., 2017). Storms also contribute to mangrove destruction through erosion and dieback, as proven by the 2007 Cyclone Ceder and the 2009 Cyclone Aila in the Sundarbans (Paul et al., 2018). In addition, sediment dynamics and topographic factors strongly influence resilience of mangrove ecosystems, with both positive (Swales et al., 2019) and negative impacts (Ward et al., 2016; Lovelock et al., 2021; Worthington et al., 2020).

Hydrodynamic forces play a critical role in building mangrove ecosystems. Recent studies have begun to quantify these influences through relevant thresholds. For example, Cannon et al. (2020) identified an 80 mm critical wave height for seedling establishment on Florida's Atlantic coast, while Constance et al. (2021) established wave power thresholds of 2.3 Wm^{-1} for stable mangrove zones and 7.1 Wm^{-1} for areas with mangrove presence in the Western Indian Ocean. Meanwhile, Kibbler et al. (2022) reported that flow velocities of 1.5 m/s and 1.2 m/s were sufficient to uproot Avicennia germinans and Rhizophora mangle seedlings, respectively. These quantitative parameters provide beneficial information for identifying suitable restoration sites. Complementary research (Lewis, 2005; Pilato, 2019; Friess et al., 2012; Le Minor et al., 2019) suggests that, while these thresholds are still being enhanced, they reflect greater attempts to establish mangrove management in hydrodynamic realities.

Despite slowing global loss trends, mangrove degradation persists (Hamilton and Casey, 2016). Effective conservation requires accurate, up-to-date spatial data (Ellison et al., 2020; Zhang et al., 2023). Field-based mapping remains challenging due to the difficult terrain, dense vegetation, and frequent tidal inundation in mangrove environments. These constraints limit regular access and data collection, making remote sensing particularly beneficial for scaled, high-resolution monitoring (Friess et al., 2019; Thakur et al., 2019). Recent advances in machine learning, when combined with multispectral inputs from open-source datasets like Landsat and Sentinel-2, have improved large-scale mangrove classification and mapping with notable accuracy (Giri, 2016; Sawant et al., 2024).

Due to these advances, the number of remote sensing studies monitoring mangrove dynamics in diverse coastal area is increasing. Some instances include southern Vietnam (Veettil et al., 2019), the Beibu Gulf (Long et al., 2022), the Indus Delta (Zhou et al., 2024), and Myanmar's Ayeyarwady Delta (Xiong et al., 2024). High-resolution imagery from QuickBird and WorldView has facilitated species-level assessments as seen in the Caribbean Coast of Panama (Wang et al., 2004) and the Texas Gulf Coast (Everitt et al., 2007). At a global scale, mangrove forest area has been delineated using Landsat-based datasets, such as Mangrove Forests of the World (Giri et al., 2011) and Continuous Global Mangrove Forest Cover for 21st Century (Hamilton and Casey, 2016), and the most recent Global Mangrove Watch v4.0 scored 95.3 % accuracy with Sentinel-2 (Leal and Spalding, 2024).

While global mangrove mapping is growing rapidly, Myanmar remains underrepresented in the literature. Despite having the third-largest mangrove area in Asia (Spalding, 2010), Myanmar receives fewer research papers than countries with smaller areas, such as Vietnam or the Philippines (Gerona-Daga & Salmo III, 2022). This gap highlights the relevance of studying the Yangon Estuary, part of the broader Ayeyarwady Delta system, formerly Myanmar's most extensive mangrove region. Reports suggest that nearly 72 % of mangroves in the Ayeyarwady Delta have already been disappeared (Aung, 2022). Despite its ecological and socio-economic significance, the Yangon Estuary has received limited focused study. Moreover, while mangrove expansion is globally rare in recent decades, signs of recovery and gain in parts of the Yangon Estuary present a valuable opportunity to understand localized drivers of resilience and change.

Thereafter, this study aims to: (1) assess spatial and temporal changes in mangrove area along the Yangon Estuary, (2) examine multi-decadal shoreline migration of mangrove fronts, and (3) identify key drivers of mangrove gain and loss. The findings will deliver baseline knowledge to inform sustainable management, particularly as mangrove expansion remains an uncommon trend globally, making recent gains in this region scientifically significant.

2. Materials and methods

2.1. Study area

The Yangon River Estuary, situated in southern Myanmar in the Yangon Region, is the easternmost distributary of the Ayeyarwady Delta complex. The Myitmaka River, later known as the Hlaing River, joins tributaries such as the Pan Hlaing River, Pazundaung Creek, Bago River, and Twante Canal. They collectively form a wide and shallow watercourse that empties into the Gulf of Martaban (Gulf of Mottama) (Fig. 1). The estuary hosts the Yangon Port, a major maritime gateway for national trade, and has undergone considerable sedimentation and morphological change.

The northern Indian Ocean, which covers the Gulf of Martaban and the Andaman Sea, is controlled by the seasonally reversing Asian monsoon (Wyrtki, 1961). The northeast (NE) monsoon, December to February, creates average wind speeds of 15–29 km/h, whereas the southwest (SW) monsoon, mid-May to September, generates stronger winds of up to 30 km/h (Liu et al., 2020). According to data from Myanmar's Department of Meteorology and Hydrology (2010–2015), Yangon has an annual rainfall of roughly 2800 mm, with noticeable seasonal change characteristic of a tropical monsoon climate (JICA, 2016).

Tidal motion in the Gulf is semi-diurnal (Sindhu and Unnikrishnan, 2013) with a range of 4–7 m according to the Indian *Tide Tables 2002* (2001). The estuary is exposed to tidal asymmetry, with shorter and steeper flood tides. High current speeds of up to 3 m/s are observed in the northern Andaman Sea (Ramaswamy et al., 2004). Seasonal waves, formed due to monsoon winds, are most intense during the southwest monsoon and weakest during the northeast monsoon (Besset et al., 2017).

Seasonal river flow runoff and tidal processes significantly influence on sediment transport in the Yangon Estuary. While monsoon season records seaward-directed flow, dry season floods compel landward sediment movement, and transport is higher during spring tides (Sir Alexander Gibb and Partners, 1974; Nelson, 2000). Suspended sediments are predominantly fine silt, and concentrations are widely varying during the wet and dry seasons, increasing considerably in the latter. June sediment levels of 2500 mg/L and October sediment levels of 5300 mg/L were recorded under the latest offshore observations conducted by JICA (2016) in 2015. Despite these observations, the broader dynamics of sediment dispersal into the Gulf of Martaban remain relatively underexplored.

In recent years, the estuary's delta front has attracted growing interest for coastal and environmental management owing to ongoing high sedimentation, mangrove development, and extensive mudflats. Fig. 1 outlines the estuarine setting, major tributaries, and the location of designated mangrove zones. Efforts to leverage natural infrastructure and greenbelt strategies have resulted in the designation of several previously unprotected mangrove stretches as protected since 2015, especially on the east coast. As part of Myanmar's coastal resilience initiatives along the Gulf of Martaban, approximately 23,855 acres (about 9653 ha) of community-managed mangrove forests have now been established along the Yangon Region coastline (Ministry of Information, Myanmar, January 7, 2024).

2.2. Materials

To map the interannual spatial distribution of mangrove forests, all available Landsat time-series imagery (Path 132, Rows 48–49) with less

Fig. 1. Location of Study Area. A: Location of Myanmar. B: Map of Yangon River Estuary and its associated rivers. C, D: Detailed Google Earth Maps of West and East Coasts, respectively, with Protected Areas designated by Forest Department, Myanmar.

than 50 % cloud cover from 1988 to 2023 were acquired via Google Earth Engine (GEE) (https://earthengine.google.com). The dataset included imagery from Landsat 5 TM (1988–2011), Landsat 7 ETM+ (2012–2013), Landsat 8 Operational Land Imager (OLI) (2013–2023), and Landsat 9 OLI-2 (2021–2022), all sourced from Collection 1. Cloud-contaminated pixels—including clouds, cirrus, shadows, and atmospheric haze—were removed using the Fmask algorithm based on the image quality assessment (QA) band. The filtered imagery was used to generate annual median composite images, ensuring consistent and accurate land cover representation.

Training datasets for mangrove classification were compiled using the Global Mangrove Watch dataset (https://www.globalmangrovewatch.org/) and historical high-resolution imagery from Google Earth. To incorporate tidal variability in shoreline detection, local tide tables from the Yangon River and Elephant Point—provided by the Myanma Port Authority—were utilized during the image selection process. Supplementary tidal information was obtained from Tide Tables published by the NOAA National Ocean Service, covering the Central and Western Pacific and Indian Ocean regions, as well as Admiralty Tide Tables Volume 5, which includes the South China Sea and Indonesia.

To assess potential drivers of mangrove forest change in the Yangon Estuary, multiple datasets were incorporated. These included the 1 arc-second Shuttle Radar Topography Mission (SRTM) global digital elevation model (DEM) for slope analysis, suspended sediment discharge (SSD) records from 2013 to 2023 at the Bago station provided by the Directorate of Water Resources and Improvement of River Systems, and regional sea-level rise (SLR) data from 1992 to 2023, sourced from the NOAA Laboratory for Satellite Altimetry. Additionally, monthly wave data, including direction and significant wave height for 2022, were obtained from the European Centre for Medium-Range Weather Forecasts (ECMWF).

2.3. Methods

2.3.1. Mangrove area extraction

Firstly, to distinguish landforms with different surface properties, this study selected surface reflectance from the blue, green, red, near-infrared (NIR), and shortwave infrared (SWIR) bands. Six spectral indices were calculated for classification inputs: the Normalized Difference Vegetation Index (NDVI) (Rouse et al., 1974; Tarpley et al., 1984), Land Surface Water Index (LSWI) (Chandrasekar et al., 2010; Xiao et al., 2004), modified Normalized Difference Water Index (mNDWI) (Xu, 2006), Mangrove Vegetation Index (MVI) (Baloloy et al., 2020), Normalized Difference Mangrove Index (NDMI) (Shi et al., 2016) and Enhanced Vegetation Index (EVI) (Huete et al., 2002). The following formulas were used in calculation of the above indices:

$$NDVI = \frac{NIR - RED}{NIR + RED} \quad (1)$$

$$\mathrm{LSWI} = \frac{\mathrm{NIR} - \mathrm{SWIR}}{\mathrm{NIR} + \mathrm{SWIR}} \quad (2)$$

$$\mathrm{mNDWI} = \frac{\mathrm{GREEN} - \mathrm{SWIR}}{\mathrm{GREEN} + \mathrm{SWIR}} \quad (3)$$

$$\mathrm{MVI} = \frac{\mathrm{NIR} - \mathrm{GREEN}}{\mathrm{SWIR1} - \mathrm{GREEN}} \quad (4)$$

$$\mathrm{NDMI} = \frac{\mathrm{SWIR2\text{-}GREEN}}{\mathrm{SWIR2} + \mathrm{GREEN}} \quad (5)$$

$$\mathrm{EVI} = 2.5 \times \frac{\mathrm{NIR} - \mathrm{RED}}{\mathrm{NIR} + 6 \times \mathrm{RED} - 7.5 \times \mathrm{BLUE} + 1} \quad (6)$$

Secondly, Google Earth Engine (GEE) was used to process annual Landsat composites and extract land cover classifications. The Random Forest (RF) classifier, widely recognized for its strong performance in mangrove land use classification (Farda, 2017; Kamal et al., 2019; Mondal et al., 2019; Li et al., 2019), was used to categorize land cover types including mangrove areas, non-mangrove tidal flats, terrestrial vegetation, surface water, bare land, and other land use classes. Training samples were extracted and categorized using historical Google Earth imagery and false color composite images. Finally, ArcMap 10.8 was used to handle and analyze the classified images. Geospatial tools were applied to calculate mangrove forest area, assess spatial coverage, and detect changes over time.

2.3.2. Mangrove shoreline extraction

According to Li et al. (2017), shoreline analysis is essential for comprehending delta evolution. While the shoreline is not a fixed line and therefore dynamic, it is approximated using a variety of indicators (Boak and Turner, 2005). Mangroves stand out among these being significant geological indicators in examinations of shoreline change globally (Souza Filho et al., 2006). In this study, the mangrove vegetation line was selected as the shoreline indicator due to its close correspondence with long-term coastal dynamics in tropical deltas (Long et al., 2022; Xiong et al., 2024).

Mangroves can be reliably distinguished in satellite imagery through appropriate band combinations. For example, Marini et al. (2015) highlighted the potential of RGB composites for visual mangrove delineation. Anang and Asriningrum (2019) demonstrated the effectiveness of Landsat 8's 5-6-4 (NIR–SWIR–Red) composite in separating mangrove forests from surrounding land cover. In this study, a combination of true color and false color composites, informed by such previous work, was created using Landsat imagery to facilitate manual visual interpretation. Thirteen historical mangrove shorelines were extracted by overlaying selected composite images from 1988 to 2023.

To ensure tidal consistency and minimize intertidal noise, most imagery was chosen from the dry season (November to April), and only images corresponding to similar tide levels—estimated using local tide tables from the Yangon River and Elephant Point—were selected for analysis. The prioritization of tide-controlled imagery improves spatial accuracy and consistency of shoreline delineation. In this study, extracted 1988 and 2023 shorelines were considered as the oldest and youngest shorelines to calculate the change analysis in the Digital Shoreline Analysis System (DSAS) of ArcGIS software.

To evaluate the potential contribution of shoreline progradation to vertical sediment accumulation, the average vertical sediment accumulation rate (AVSA) was estimated following the approach of Xiong et al. (2024):

$$AVSA = V \tan\theta \quad (7)$$

Where V is the average accretion rate of the shorelines, and θ is the mean slope of the area obtained from DEM.

2.3.3. Extraction of shrimp pond extent and associated mangrove loss

To evaluate human-induced mangrove degradation, shrimp pond boundaries were manually digitized from Landsat imagery at approximately five-year intervals between 1988 and 2023. Image selection was based not only on cloud cover but also on seasonal variation in pond texture, which improves visual detectability. In some cases, multi-season imagery was examined to capture textural changes over time. Shrimp ponds were identified based on distinctive geomorphological and spectral patterns—particularly their regular, rectilinear shapes and high reflectance during dry-season conditions. All digitization was conducted by a single analyst at a consistent viewing scale to ensure interpretive consistency.

Mangrove loss associated with shrimp pond expansion was quantified using spatial overlay techniques in ArcGIS 10.8. For each time interval, mangrove loss polygons—derived from classified annual mangrove maps—were intersected with the pond extent from the final year of that period. Impounded mangrove areas were extracted by overlaying the classified mangrove extent with the visually delineated shrimp pond boundaries of the same year. This approach enabled quantification of both direct mangrove conversion and enclosed mangrove degradation linked to aquaculture development.

2.4. Accuracy assessment

Classification accuracy was evaluated using a confusion matrix derived from the Random Forest classifier output in GEE. The confusion matrix serves as a foundation for quantifying classification performance and identifying potential sources of error that may inform future refinement of classification procedures (Foody, 2002). Key metrics include Overall Accuracy (OA)—the proportion of correctly classified samples relative to the total—and the Kappa coefficient, which accounts for agreement expected by chance (Congalton, 1991). Additionally, Producer's Accuracy (PA) and User's Accuracy (UA) were calculated for each land cover class, allowing class-specific assessment of omission and commission errors.

The classification results demonstrated consistently high performance, with minimum OA and Kappa values of 0.92 and 0.91, respectively, across all analyzed years. A complete summary of OA, Kappa, PA, and UA values for each class and year is provided in the Supplementary Material (Table S1). The mangrove class specifically achieved PA values above 92 % and UA values above 90 % in all years, confirming its robust separability in the classification scheme. Although some confusion was observed between certain land cover categories such as mangroves and non-mangrove tidal flats, or bare land and sparsely vegetated areas, though these errors were infrequent and did not significantly compromise the overall classification reliability. Accuracy was largely consistent across time and space, with only minor reductions in early years likely due to lower image quality and limited vegetation cover.

For shoreline movement analysis, shoreline change rate was calculated with a 90 % confidence interval in DSAS. A minimum shoreline intersection threshold of four transects was applied to enhance the statistical reliability of calculated shoreline change rates. In some early images, sparse mangrove vegetation presented challenges for precise shoreline extraction.

3. Results

3.1. Variations in mangrove forest area

The overall mangrove coverage rose from 1175.5 ha in 1988–5469.7 ha in 2023, as shown in Fig. 3A, which depicts area variance with linear regression trend lines and contributions split into two distinct eras. Mangroves along the study estuary have grown by 4294.2 ha within the last 35 years, representing 3.6 times their extent in 1988. This translates to the average annual increase rate of approximately 4.5 % along the overall coast. Nevertheless, it is important to note that this trend did not

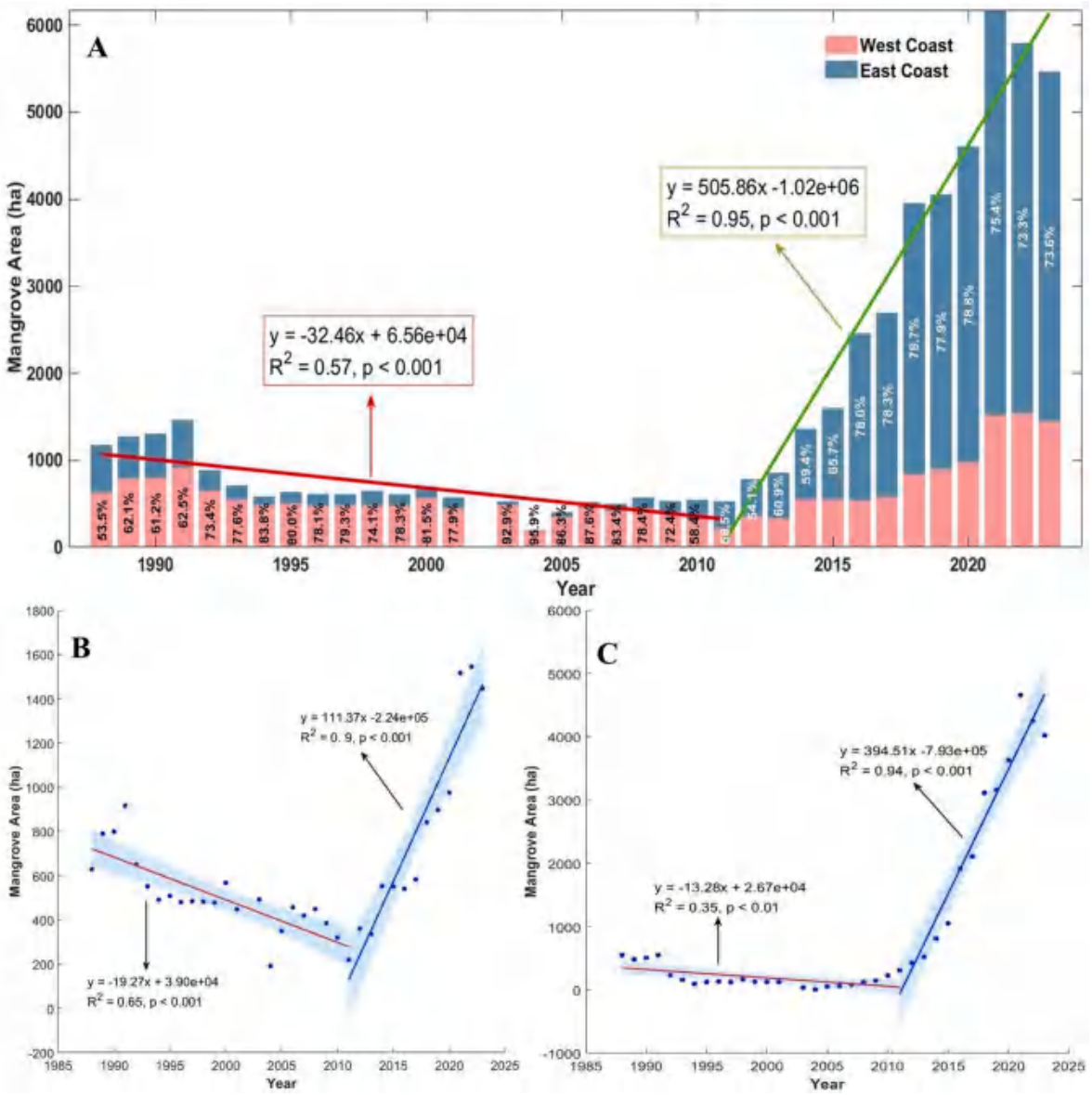

Fig. 2. Temporal variation of mangrove area along the Yangon Estuary. A: Total area from 1988 to 2023, with west (red) and east (blue) contributions. Percentages indicate the dominant coast's share (black for west, white for east). B–C: Area trends for the west and east coasts, respectively, with linear regressions and 95 % confidence intervals.

persist throughout the whole study period (Fig. 2A). Despite occasional fluctuations, the mangrove area indicated a gradual decline mainly from 1991 until around 2011, with almost half of the initial mangroves lost, opposing to the overall incline (Fig. 2A). After 2011, the mangroves experienced a dramatic increase, with the total increase amounted to 4938.7 ha, making this recent period the primary contributor to the overall increase over the 35 years. Similarly, in terms of contribution, the west coast accounted for the total coverage until 2011, after which the east coast showed significant shift (Fig. 2A). The variations of mangrove area within two separated regions presented the same patterns in general compared to the overall trend, by taking the turning point at 2011 (Fig. 2B and C).

Between 1988 and 2011, in the western region, mangroves experienced a reduction of approximately two-thirds, decreasing from 630 ha to 220.2 ha, with an average annual decline of 19.3 ha. Since 2011, this region began to increase at an average annual rate of 111.4 ha (Fig. 2B). For the eastern region, although mangrove area declined from 1988 to 2004, reaching the minimum points for all data sets, the trend line extends to 2011 as it reflects a significant increase starting from this year. In 1988, the eastern region's mangrove area was 547.5 ha, declining at an annual rate of 13.3 ha until 2011. However, after 2011, it recovered notably, reaching to a peak of 4656.2 ha by 2021, with an annual growth rate of 394.5 ha (Fig. 2C).

In summary, both coasts witnessed substantial mangrove expansion. Mangroves expanded by over 6-fold on the eastern coast and more than doubled on the western coast. Despite both regions showing expansion, the western region more closely mirrored the estuary-wide pattern in the early years, whereas the eastern region did so in the most recent years.

3.2. Gain and loss in mangrove area

Over the entire study, the two coasts revealed unique spatial patterns of mangrove area gain and loss (Figs. 3 and 4). To describe these changes, site names officially designated by the Forest Department (FD), as shown in Fig. 1C and D, will be referred. During 1988 to 1993 (Fig. 3A), mangroves were primarily concentrated along the west coast. The Green Wall (GW) region showed significant losses both landward and seaward sides, while Mya Sein Thaung (MST) recorded minor gains,

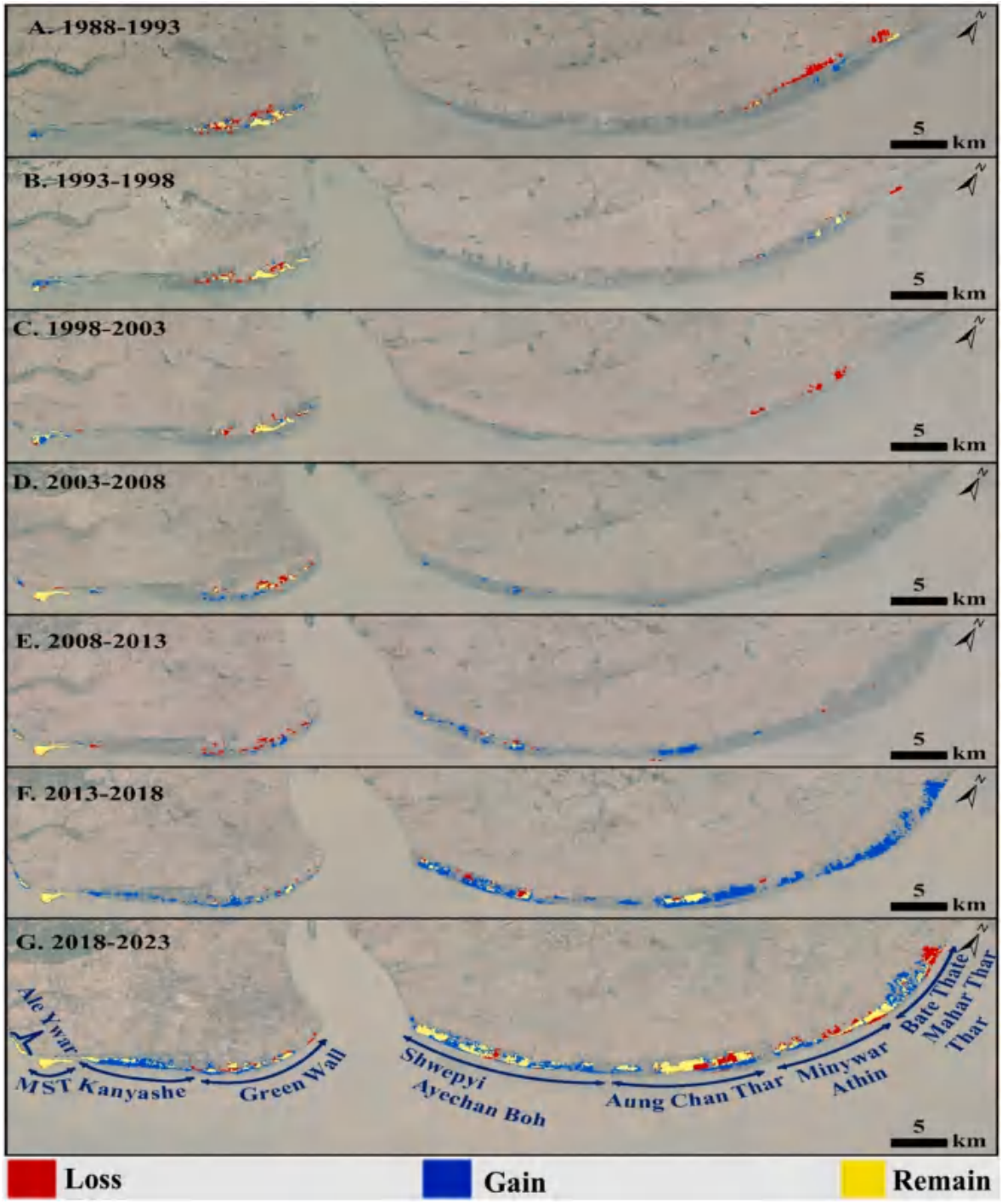

Fig. 3. Gains and losses of mangrove area in the study area. A–G: Spatial distribution of mangroves during 1988–2023. Remaining area means the extent in the initial year of that period.

totaling gain and loss amount of 189.2 ha and 267.7 ha, respectively. On the eastern coast, mangroves that were once confined to what are now known as Minywar Athin and Bate Thate Mahar Thar Thar were nearly vanished by 1993, resulting in a total loss of 464.6 ha, with only a minor seaward gain of 78.4 ha.

From 1993 to 1998 (Fig. 3B), MST growth on the western coast mainly contributed 155.6 ha of gain while GW primarily drove depletion, resulting a regional loss of 224.6 ha. The east coast remained largely unchanged, with minimum gains (75.5 ha) and losses (64.9 ha) effectively balancing each other. Between 1998 and 2003 (Fig. 3C), the west coast experienced ongoing GW depletion, MST growth, and the establishment of the Ale Ywar region (ALY). These produced nearly balanced net changes of 161.5 ha gained and 151.9 ha lost. MST showed some seaward losses, likely linked to exposure to southwestern monsoon-driven wave action. Meanwhile, on the east coast, nearly all mangroves diminished, depicting 35.5 ha gained and 168 ha lost (Fig. 4).

Within 2003–2008 period, persistent areas in GW region began to deplete after 15 years of stability while MST and ALY remained relatively stable (Fig. 3D). The east coast began recovering, with new emerged patches as gains totaled 115.4 ha, while losses declined to just 28.6 ha. Based on Fig. 3E, the 2003–2008 period revealed similar trends

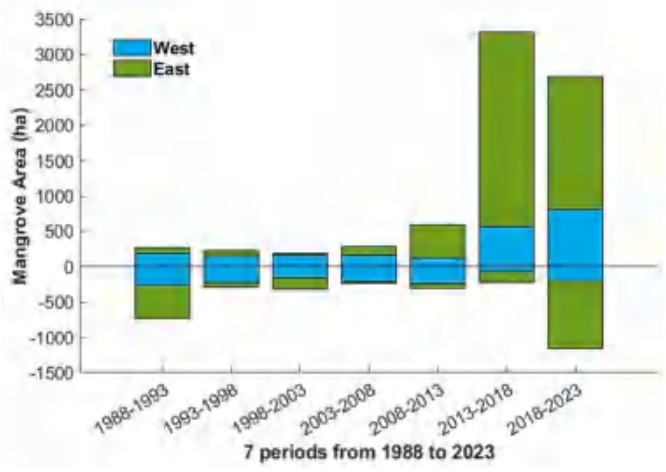

Fig. 4. Loss and gain areas of the seven periods in west and east coasts.

for the west coast, while ALY expanded further upstream, likely aided by its sheltered setting and local sediment trapping. Meantime, the east coast demonstrated notable growth, particularly in Aung Chan Thar and Shwepyi Ayechan Boh areas, contributing to a total gain of 463.9 ha.

Between 2013 and 2018 (Fig. 3F), substantial growth of the Kanyashe and recovery of GW region led to minimum local loss of 61.6 ha throughout the west coast. On the eastern side, dramatic seaward and lateral expansion occurred, totaling 2755.2 ha, six times the previous period, transforming the coastline and establishing the foundation of building a green belt for coastal protection. Recently, from 2018 to 2023 (Fig. 3G), despite increased losses, the west coast recorded its peak gains of 799.8 ha, driven by continued seaward advances. Similarly, the east coast continued to expand, with a remarkable mangrove growth of 1892.6 ha. However, this expansion was accompanied by a significant near-half loss of 973.5 ha (Fig. 4). FD's announcements stated that the new mangrove forests emerged naturally after 2008, aligning with the findings presented in Fig. 3E. In summary, while early decades were marked by losses, particularly in GW of the west and across the eastern coast, the recent decade has seen significant recovery and expansion, especially on the eastern coast.

3.3. Mangrove shoreline changes

Based on the shoreline analysis of 944 transects, the majority of mangrove shorelines migrated seaward over the previous 35 years, with an average rate of 58 ± 3.2 m/yr, however, certain coastal areas showed landward movement (Fig. 5). Remarkably, approximately 92 % of the shoreline expanded seaward, resulting in accretion and erosion rates of 63.9 m/yr and −18.4 m/yr, respectively. Additionally, the maximum movement between the oldest (1988) and the youngest (2023) shorelines along the entire coast amounted to −348.3 m for erosion and 4502.2 m for accretion.

Over 35 years, both western and eastern coasts have been accreted with overall rate of 32.7 ± 2.9 m/yr and 71.6 ± 3.8 m/yr, respectively (Fig. 6). With average rates of +35.6 m/yr for accretion and −1.7 m/yr for erosion, seaward progradation controlled 92.2 % of the Yangon River estuary's western coast, with little to no substantial erosion occurring (Fig. 6A). Similar to this, the eastern coast showed significant accretion, making up 92.3 % of the region; though, the average rates of change were quite distinct, with erosion occurring at −29.1 m/yr and accretion at +79.6 m/yr (Fig. 6B). The easternmost area of the eastern region exhibited the highest erosion, with a peak rate of −56.7 m/yr. Thus, both regions exhibited substantial seaward mangrove encroachment, consistent with the spatial patterns described in Section 3.2 and aligning well with the documented accretion trends in the eastern Ayeyarwady Delta reported by Anthony et al. (2019) and Chen et al. (2020). Despite considerable expansion, the mangrove growth along the Yangon River estuary was scattered, contributing to irregular and uneven shorelines in

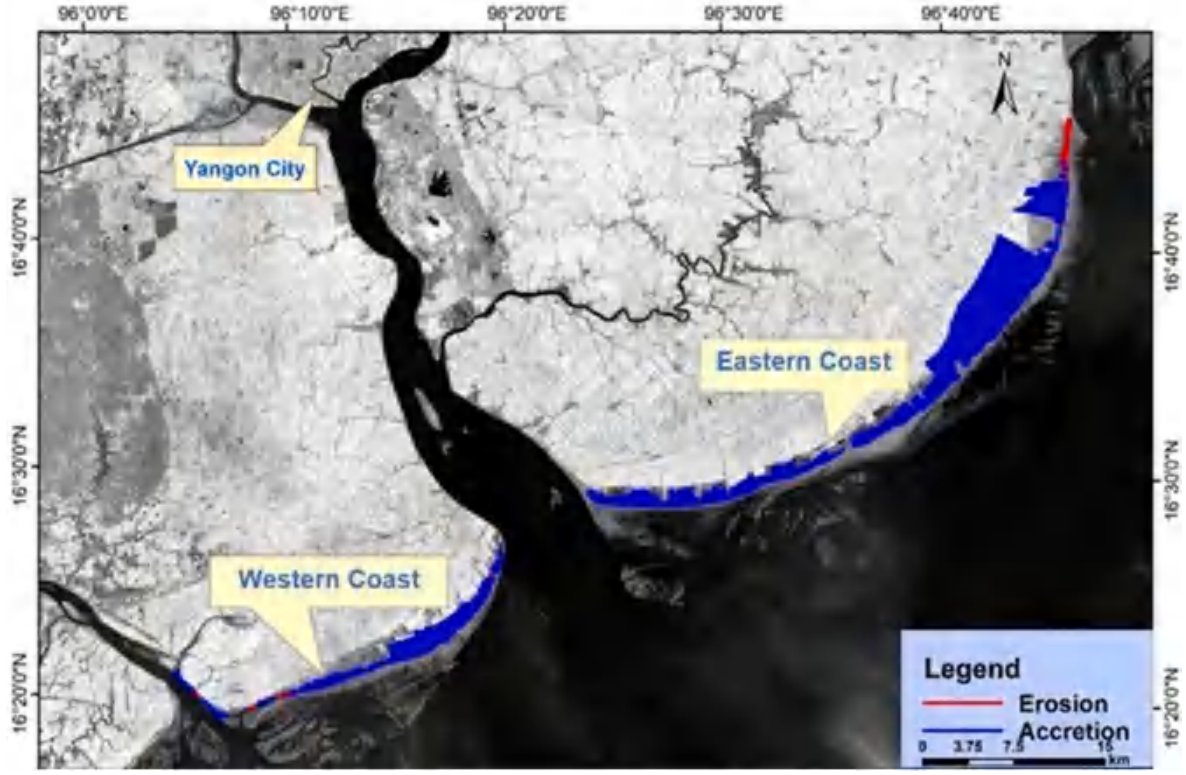

Fig. 5. Mangrove shoreline movement along the Yangon Estuary showing accretion (blue) and erosion (red) along the western and eastern coasts. Key regions and divisions are labeled.

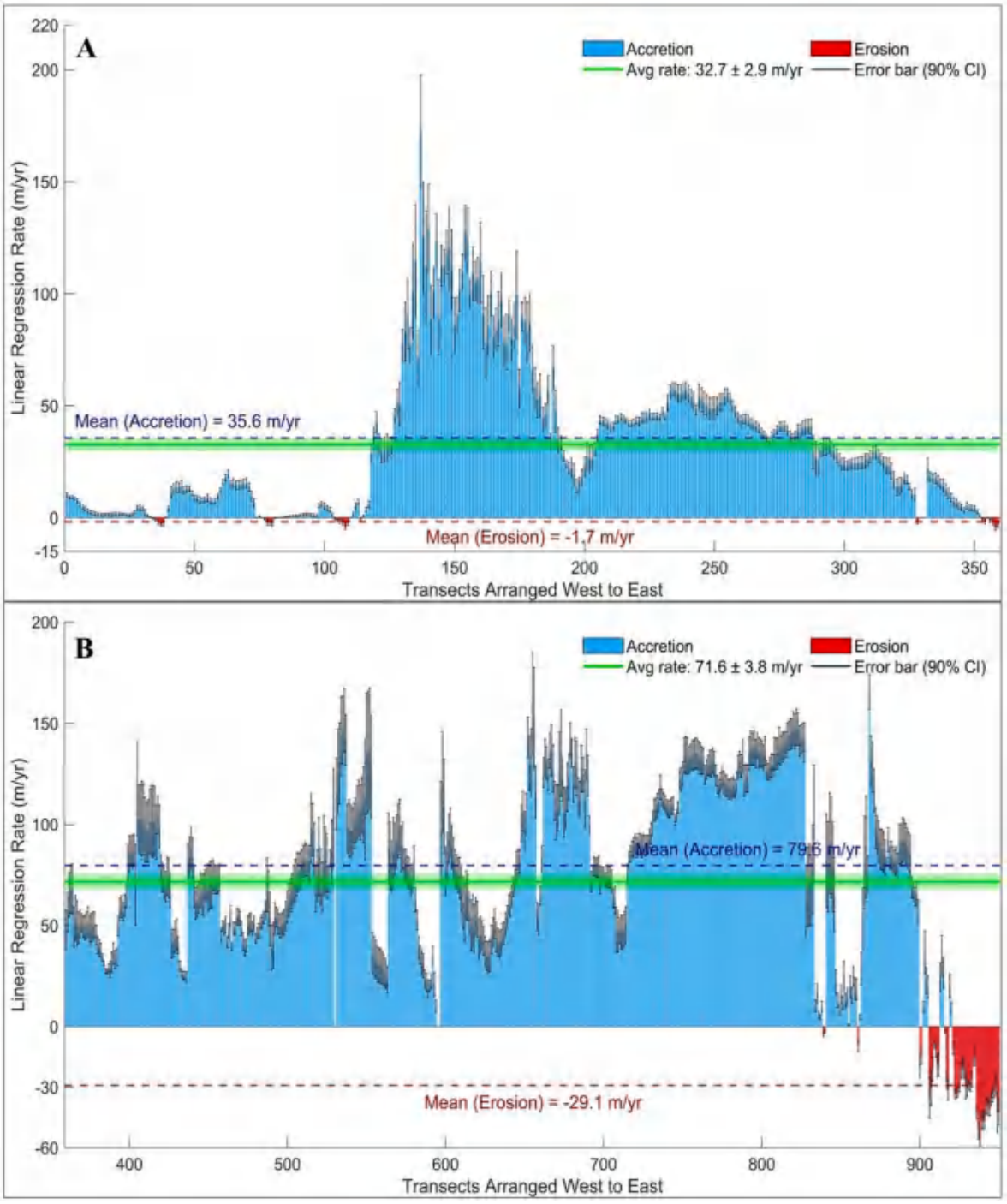

Fig. 6. Transect-based linear regression rates (LRR) of mangrove shoreline change. Bars represent individual transects for the western (A) and eastern (B) coasts, with error bars indicating 90 % confidence intervals.

the early years.

3.4. Patterns of mangrove degradation linked to shrimp aquaculture

The impact of shrimp pond development on mangrove loss was quantified by visually extracting shrimp pond boundaries and mangrove extent within those ponds over a five-year interval (Fig. 7). Between 1988 and 2008, the proportion of mangrove loss directly attributed to shrimp pond construction in the region was relatively low, with losses from pond construction accounting for less than 10 % (Fig. 7A). This changed significantly after 2008. From 2008 to 2018, the proportion of mangrove loss within shrimp pond areas has increased dramatically, peaking at nearly 65 % of total loss during this period, before decreasing again in the most recent interval (2018–2023), most likely due to external factors such as the COVID-19 pandemic and political instability.

Concurrently, since 2008, mangroves have been bunded in the extensive traditional "trap and hold" shrimp farms (Fig. 7B). These in-pounded mangroves in the shrimp farm areas have been significantly increasing during the last decade and occupied nearly 30 % of the entire area of mangroves by 2023. The regression analysis reveals a statistically strong expansion trend, with shrimp pond areas increasing at an estimated rate of 120 ha/yr ($R^2 = 0.95$, $p < 0.001$), and in-pounded

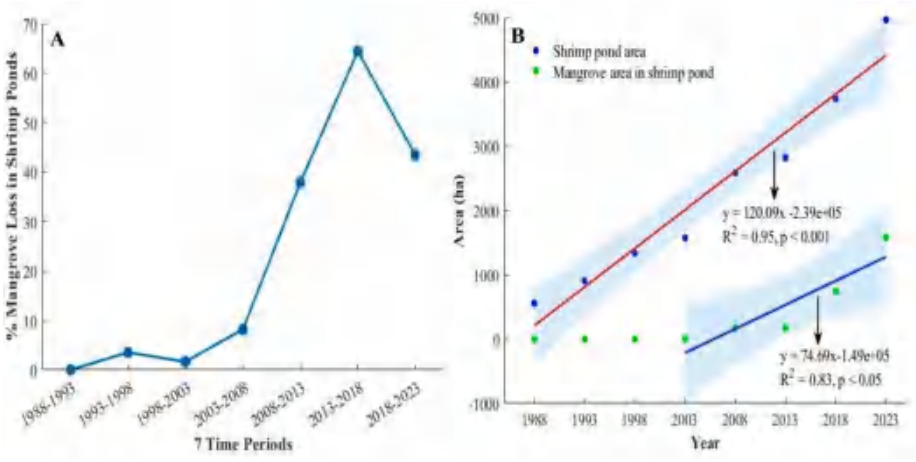

Fig. 7. A: Percentage of mangrove loss in every period by shrimp ponds. B: Shrimp Pond areas and impounded mangrove area extracted visually by 5-year interval.

mangrove areas expanding at approximately 75 ha/yr ($R^2 = 0.83$, $p < 0.05$). These trends suggest significant land use transitions over the past decade.

4. Discussion

4.1. Sediment dynamics and mangrove expansion

4.1.1. Impacts of fluvial sediment supply

Suspended Sediment Discharge (SSD) from rivers is crucial for forming tidal flats in deltas, creating essential habitats for mangrove establishment (Swales et al., 2019). While some studies associate declining riverine SSD with slowed expansion or even losses of deltaic mangroves (Worthington et al., 2020; Lovelock et al., 2021; Jayanthi et al., 2023), others, such as recent research in the northern Beibu Gulf, suggest that reduced SSD did not directly constrain mangroves forest expansion (Long et al., 2021). Due to limited availability of long-term sediment records in Myanmar, SSD data from the Bago River at the Bago station (2013–2023), provided by the Directorate of Water Resources and Improvement of River Systems, were analyzed to infer potential influence on the estuary. This annual average SSD data suggest a statistically significant increasing trend, with a linear regression slope of approximately 614.5 kg/s annually ($R^2 = 0.48$, $p < 0.05$), despite upstream damming activities. Pearson's correlation analysis further revealed a moderate but significant positive correlation between SSD and mangrove area expansion across the estuary ($r = 0.64$, $p = 0.03$), and separately for the western ($r = 0.68$, $p = 0.02$) and eastern ($r = 0.62$, $p = 0.04$) coasts. These results suggest that fluvial sediment input—particularly from the Bago River—supports mangrove growth, with stronger correlation noted on the west coast. These results suggest that fluvial sediment input, particularly from the Bago River, supports mangrove growth, with stronger correlation noted on the west coast. However, various analyses, including sediment composition, distribution, and seasonal flux, should be conducted along the coast for better understanding. However, this conclusion is drawn from a single monitoring station and may not represent the full sediment budget of the estuary, which receives inputs from multiple river systems. Thus, the findings should be interpreted as indicative rather than exhaustive. This trend of increasing SSD aligns with the long-term seaward progradation of mangrove shorelines observed in Section 3.3.

4.1.2. Influence of estuarine deposition distribution

Previous field reconnaissance by Anthony et al. (2019) revealed a west-to-east gradient in shoreline morphology and sediment composition across the Ayeyarwady Delta, with sediment becoming increasingly muddy toward the Gulf of Martaban. Although most of their study was focused on the western delta, there was a single station in the eastern section near Yangon that, with a median size of approximately 180 μm, indicating a finer sedimentary environment favorable for mangrove colonization. Supporting this, the 2002 soil map by the Land Use Division of the Myanma Agriculture Service (as cited in Lwin and Khaing, 2012) indicates the presence of mangrove forest soils along the coastline of Yangon estuary (Fig. 8). Similarly, Park (2004) also found that greater mud content provides a greater amount of nutrients for plant growth, possess a greater mangrove cover, whereas cleaner sands and lower mud content, typically in open positions, support fewer mangroves. Combined, these observations suggest that the environments in the Yangon estuary's soils and sediments are conducive to mangrove establishment and contribute in part to the recent expansion trend reported in this study.

4.1.3. Proximal sediment sources and transport

Another peculiar feature of this estuary is the presence of large sediment sources on the sea side (Glover et al., 2021; Whitty and Maw, 2023). Recent studies showed that Approximately 83 % of sediment from the Ayeyarwady River is carried eastward into the Gulf of Martaban rather than deposited at the river mouth (Kuehl et al., 2019; Liu et al., 2020). In addition, estuarine exchange of turbid water from the northeastern Gulf of Martaban facilitates sediment import into the estuary (Glover et al., 2021). Moreover, rapid muddy bank erosion in the Sittaung River estuary (Shimozono et al., 2019; Liu et al., 2020) may also contribute to the muddy foreshore deposit along the accreted east coast to some extent.

Meanwhile, due to coastal orientation, shallow coastal morphology, and with the timing of energetic seasonal marine conditions, Yangon estuary has possibly high sediment retention (Glover et al., 2021). Within the Gulf, tidal currents dominate as the primary drivers of sediment resuspension reworking (Kuehl et al., 2019). Tidal cycles further regulate sediment transport, with seaward transport during ebb tides and potential landward redistribution during flood tides (Harris et al., 2022), supporting accumulation in intertidal zones. This interaction of tidal forces, estuarine exchange, and coastal circulation can foster the formation of mud flats and nutrient-rich soils that support mangrove establishment and expansion in the study area.

4.2. Environmental challenges

4.2.1. Impacts of extensive tidal flats

The evolution and existence of extensive tidal flats along the coast (Fig. 9B) plays an important role in mitigating wave energy, effectively attenuating wave action along nearby shoreline. Although direct elevation measurements of these tidal flats remain limited, the

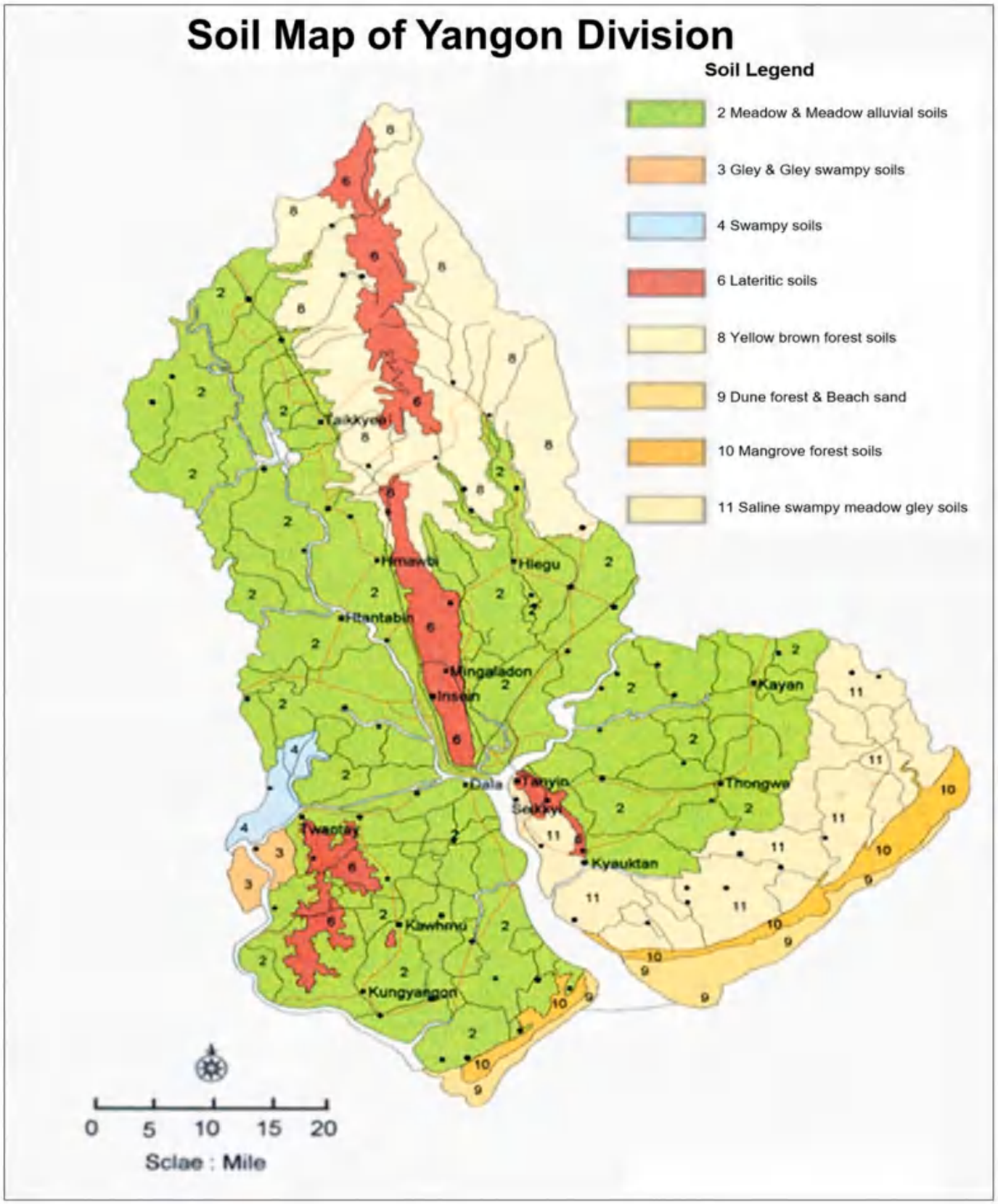

Fig. 8. Soil map of the Yangon area (copyright of Land use division, Myanma Agriculture Service (Feb 11, 2002). Adapted from Lwin and Khaing (2012), p. 177.

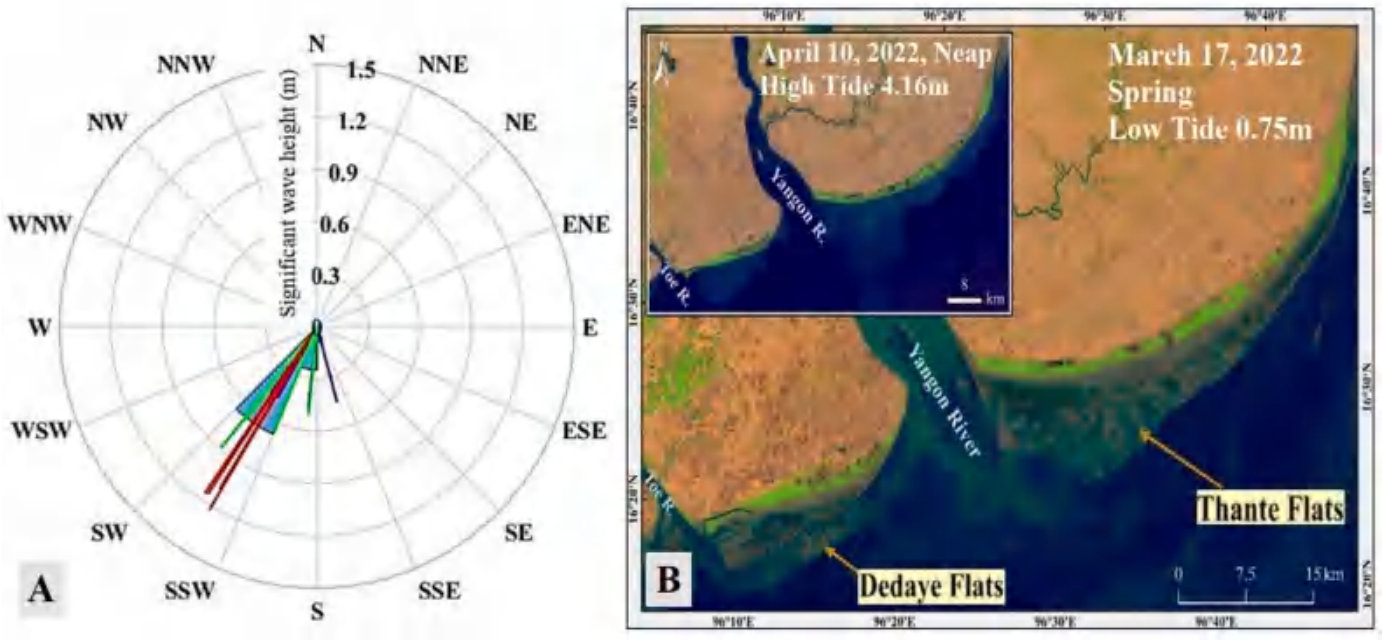

Fig. 9. A: Monthly significant wave height and direction in the Yangon Estuary for 2022, derived from ECMWF reanalysis data. B: Presence of extensive tidal flats along the estuary, which are submerged at high tide and exposed at low tide. Local names are shown as recorded in historical charts.

nearshore morphology along Yangon coast is possibly to have accretional processes vertically and laterally. This inference is supported by observations of shallower waters and high sedimentation within the offshore channel of Yangon River (JICA, 2016). In the case of the Kanyashe mangrove development, the sandy beach has gradually transformed into a low-energy depositional environment dominated by silt and muddy sediments, evolved into saltmarsh over time and thereafter, being replaced by mangroves (Source: local news). While direct observations are lacking, long-term residents interviewed during the study described noticeable changes in local nearshore conditions, including shallower depths, declining wave intensity at the beach, and the visible formation of offshore flats approximately one mile from the coast since the early 2000s. As seen in Fig. 9B, the flat along the west coast appear as segmented and detached units, which can additionally shelter and buffer the main coast against offshore forces locally, meanwhile, particularly the extensive, continuous muddy flats along the east coast create a favorable substrate for mangrove establishment and expansion, as observed in northern Beibu Gulf (Long et al., 2022).

4.2.2. Impacts of waves

Wave activity is a one of the key drivers of shoreline erosion, a process projected to intensify under climate change scenarios (Gilman et al., 2008). Simultaneously, fringe mangroves, particularly those in shallow coastal waters, are highly vulnerable to wave-induced stress and erosion (Sakho et al., 2011; Hu et al., 2015). Wave action is reduced in the Gulf of Martaban (Kuehl et al., 2019). The region is influenced by the southwest monsoon with southwest waves (Fig. 9A), resulting in uprooting and loss of mangroves, particularly the erosion observed in the southwest part of MST (Fig. 3; Fig. 12C). Even during the dry season, with wave heights 0.5–1.0 m, persistent wave action can hinder the initial establishment and growth of marsh and mangrove ecosystems along the shoreline. On the one hand, small waves (with significant wave height less than 20 cm) are capable of resuspending sediment over tidal flats (Green, 2011; Uncles and Stephens, 2000) thereby potentially increasing sediment availability to adjacent wetlands. On the other hand, wave forecasting and hindcasting, and observational data from 2015 (JICA, 2016) further demonstrated that waves at the Yangon River offshore are characterized by long period waves, even the wave heights are low. In general, long period waves hold higher energy to mobilize seabed materials, thereby, resulting changes in geographical features, followed by impacts on morphological evolution in mangrove ecosystems. Therefore, although the region is more sheltered and calmer from the wave action compared to the Ayeyarwady delta, generally small but long-period waves, with possible sediment reworking and redeposited along the coast, can further foster the mangrove development.

4.2.3. Impacts of cyclone disturbance

The Bay of Bengal frequently experiences tropical cyclones, with Myanmar situated in their path, over 25 of which have affected the Ayeyarwady delta since 1870 (Knapp et al., 2010). Among them, the 2008 Cyclone Nargis stands out as the most destructive in recent history, and the only cyclone since 1968 to directly strike both the Ayeyarwady and Yangon regions (Gunasekera et al., 2023). While cyclones often cause widespread destruction, they may also contribute to mangrove resilience by depositing suspended particulate matter (SPM) and allochthonous sediment that enhance surface elevation—a critical mechanism for coping with sea-level rise (Smoak et al., 2013; Ward et al., 2016). Following Nargis, sediment concentrations remained elevated for at least two months, possibly, due to unusually high fine-grained fluvial sediment inputs (Besset et al., 2017). The most severe impacts were recorded in the exposed western delta. In contrast, the Yangon estuary, located on the more sheltered eastern side, experienced relatively less damage due to the storm's inland trajectory. This underscores the spatial variability in cyclone effects across the delta. In the years following Nargis, signs of ecological recovery were evident. Notably, from 2011 onward, significant lateral and seaward expansion of mangroves was observed in the eastern estuary (Fig. 3D–E). This expansion may have been aided by cyclone-driven dispersal of seeds and propagules across barriers, at greater scale than what occurs under normal tidal conditions (Peterson and Bell, 2015). Although causality cannot be fully confirmed, these observations suggest that Cyclone Nargis may have indirectly supported longer-term mangrove regeneration. However, such effects are highly localized and cannot be generalized to all future storm events.

4.2.4. Impacts of sea level rise

Sea level rise is recognized as a significant threat to mangroves, as it can alters inundation patterns and salinity levels (Ball, 1988; Friess

et al., 2012) leading to long term adversely effect on the extent and health of mangrove ecosystems globally (Lovelock et al., 2015, 2017; Kassakian and Friedman, 2017). Considering global and regional influences, sea level in 2100 is projected by the latest IPCC (2021) to rise up to 96 cm (SSP2-4.5 scenario) and up to 123 cm (SSP2-8.5 scenario). Consequently, the extensive, low-lying Ayeyarwady/Yangon Deltaic regions are particularly vulnerable to sea-level rise as 0.5 m sea level rise would result in the shoreline along the Ayeyarwady Delta retreat of 10 km (Myanmar NAPA, 2012). However, mangroves demonstrate remarkable resilience to fluctuations in sea level (Woodroffe and Grindrod, 1991; Alongi, 2015) due to their ability to actively modify their environment through surface elevation change processes facilitated by various mechanisms (Furukawa and Wolanski, 1996; Ward and Drude de Lacerda, 2021). In this study, annual mean sea level anomalies from 1992 to 2023 were derived from NOAA satellite altimetry datasets. Despite spatial variability in sea level trends near Yangon (Chen et al., 2020), the long-term linear trend based on this dataset reflects a statistically significant regional rise of approximately 3.24 mm/year (Fig. 10). Meanwhile, the average vertical sediment accumulation rate along the Yangon estuary, calculated from the average slope, is 64.7 cm/yr. Thus, the moderate regional SLR rate appears to be balanced by the relatively rapid sediment built-up in the estuary. While mangrove responses to relative sea-level rise are complex and site-specific, the observed balance between steady vertical accretion and the abundant fine sediment supply from the Gulf of Martaban suggests that, at present, the mangrove shorelines in the Yangon Estuary, are keeping pace with rising seas, enabling continued seaward expansion.

4.3. Impacts of anthropogenic activities

4.3.1. Threats

Historical policies and land concessions laid the groundwork for large-scale land use transformation in the Yangon Estuary. In the 1990s and early 2000s, tens of thousands of acres of land were granted as concessions for aquaculture and industrial-scale paddy cultivation, following the completion of water control infrastructure for paddy cultivation and the 1989 passage of Myanmar's Aquaculture Law (Belton et al., 2017). As part of special government program, three shrimp culture zones were established within Yangon region between 2000 and 2006. Among these, Zone No.2 lies along the east coast of the Yangon estuary, initiated in 2001 (FAO, 2003). However, as shown in Fig. 7A, shrimp pond development accounted for only a small proportion of mangrove loss until 2008. Thus, the primary drivers during that period were likely agricultural expansion, salt pans, and domestic fuelwood harvesting, mirroring national trends reported in other mangrove regions of Myanmar.

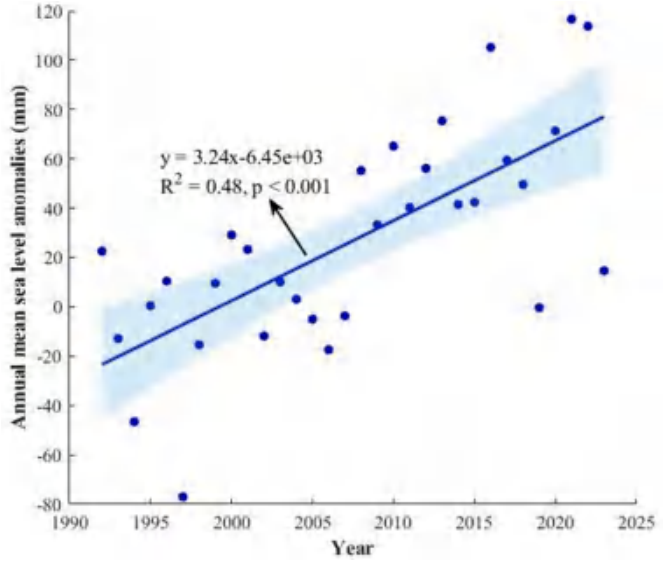

Fig. 10. Annual mean sea level anomalies for the Yangon region, based on NOAA satellite altimetry from 1992 to 2023. A linear trend shows a statistically significant sea level rise of approximately 3.24 mm/yr.

Following 2008, a marked shift occurred. Shrimp pond development rapidly became the dominant driver of mangrove degradation during 2008–2018. According to Whitty and Maw (2023), rice field conversion is the main cause of mangrove degradation in the Gulf of Martaban, which contradicts the findings of this study. However, interviews with local stakeholders and mangrove restoration project leaders support the finding that shrimp ponds, not agriculture, are the leading cause of recent mangrove decline, with domestic fuel having relatively lesser impact.

In addition, traditional shrimp farms have increasingly retained mangrove patches within their pond systems (Fig. 7B). While initially left standing, these "in-pounded" mangroves (now about 30 % of all mangrove extent) often degrade over time due to altered hydrological conditions caused by bunding. Field reports and local accounts confirm decomposition and dieback of these trees due to root suffocation and stagnant water, as previously documented in national assessments (FAO, 2003). Recently, several issues and concerns have arisen among different stakeholders regarding the shrimp farm models in mangrove areas. Therefore, the findings underscore that it is likely that without careful management, the mangrove ecosystems in the region will face a concerning decline.

Globally, overgrazing by goats and camels is a common disturbance, particularly in Middle Eastern regions, highlighting the broader implications of livestock grazing management on mangrove sustainability (Lewis, 2006). Along Yangon Estuary, livestock grazing, though a lesser threat compared to other challenges, also poses notable risks to seedling establishment in restored or naturally regenerating areas. In some zones, especially around saltmarshes and mangrove plantations, buffalo grazing results in trampling and consumption of young mangrove seedlings, hindering their establishment and growth (Fig. 11B). In contrast, positive examples such as the community-led protection of Aleywar's saltmarsh zones suggest that grazing control can significantly improve restoration outcomes (personnel communications).

Finally, while potential developments like the Yangon Port expansion into the sea could pose a potential future threat, current throughput trends and underutilized capacity suggest that such developments are unlikely in the near term (Myanma Port Authority).

4.3.2. Conservation and management

Research and restoration efforts targeting mangrove ecosystems in Myanmar have gained new momentum following the 2010 political reforms (Veettil et al., 2018). This shift in environmental governance likely contributed to the noticeable post-2011 increase in mangrove coverage observed in this study (Fig. 2A). Restoration initiatives have been conducted in Yangon region as of being one of 13 districts where mangroves, both dense and sparse, are still present. Based on the collected past legal process's records, a major restoration project was launched in 2011, covering 22 villages along the Yangon coast. The organization named "Mingalar Myanmar" planted 293,833 saplings along the eastern coast by the end of 2011. However, due to land tenure uncertainties and the lack of legal registration after planting, portions of these restored areas were subsequently converted to other land uses. Recent Myanmar Reforestation and Rehabilitation Plan (2018–2027) by the Forest Department aims to restore nearly 29,690 acres (approximately 12015 ha) of mangroves across degraded and depleted areas, targeting 3000 acres (1215 ha) annually over Myanmar coast (Aung, 2022). Although the overall effectiveness of these plantation programs remains to be fully assessed, feedbacks from local interviews and Forest Department officials indicate promising results in the Yangon region. Efforts by several organizations such as the Gulf of Mottama Project (GoMP), World View International Foundation (WIF), and the

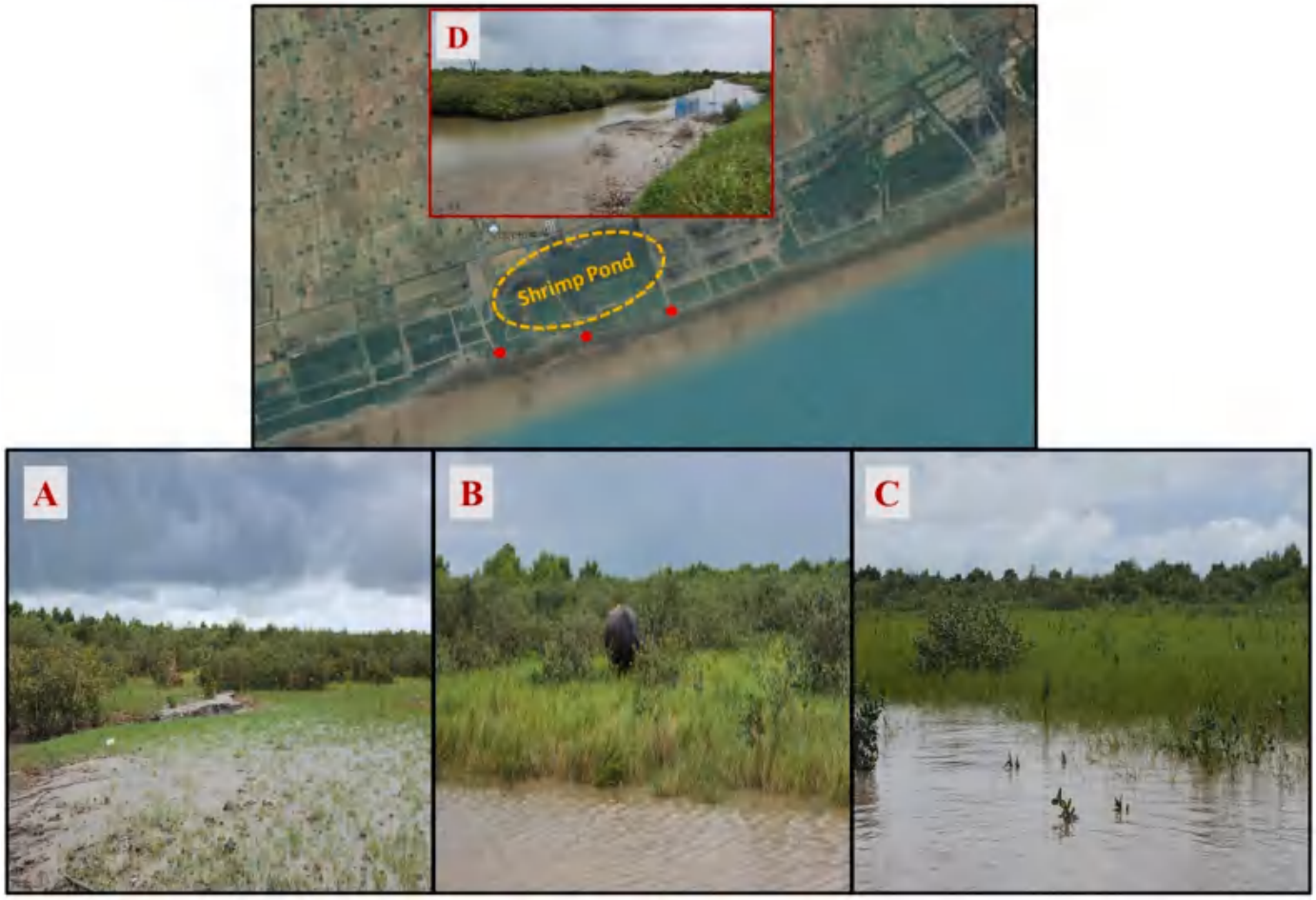

Fig. 11. Pictures of field observation area in eastern coast. A, B, C: Naturally encroached mangroves along the coast. D: Recently cultivated shrimp pond in the area compounded mangroves inside and remnants of old mangroves can be seen inside. (Red dots show positions of A, B and C).

Biodiversity and Nature Conservation Association (BANCA), are actively engaging in mangrove conservation along the coast, through awareness campaigns, youth training and ecosystem restoration. As a result, local stakeholders now have fairly sufficient awareness and attributes to active participation in mangrove restoration although engagement levels still vary across stakeholder groups. However, despite these encouraging efforts, significant challenges still persist, due to the fragmented governance among government departments hinders coordinated land-use planning and decision making. Strengthening inter-agency collaboration and robust enforcement of conservation policies will make rooms in addressing these issues and sustaining mangrove recovery efforts in the long term.

5. Conclusions and recommendation

Findings from satellite imagery and field observations indicate that the Yangon coastline is predominantly characterized by accretion, with substantial seaward mangrove expansion on the newly accreted tidal flat. The overall trend was mainly influenced by the west coast until the mid-2000s, after which the east coast began to play a more dominant role in shaping the patterns of the mangrove growth. Despite the continued increase in mangrove coverage after 2011, recent years have shown signs of decline in total mangrove extent, pointing to a potential reversal in gains and underscoring growing anthropogenic pressures on ecosystem sustainability. Among these pressures, aquaculture expansion, particularly shrimp pond construction and bunding, has emerged as the dominant driver of mangrove loss in the region.

From a geomorphological perspective, mangroves in the Yangon Estuary appear to be resilient to natural factors such as sea-level rise and localized subsidence. This resilience is supported by sedimentary processes including sediment reworking and remobilization under long-period waves, dominant tidal forcing, and the presence of extensive accreting tidal flats as all of which provide a stable foundation for mangrove establishment. Given by the region's physical setting and the past event, less destructive impacts from tropical cyclones are expected for the regional mangroves in the future. On a landscape-scale, natural disturbance was of a much lower magnitude compared to large-scale human-driven loss. If left unchecked and uncontrolled, mangrove removal could be a serious concern for erosion in the mud-dominant estuary coast.

To ensure effective mangrove restoration, it is essential to strengthen law enforcement, establish continuous monitoring, and promote inter-agency coordination. Sustainable agriculture and aquaculture practices should be encouraged, alongside proactive management of unregulated development, pollution, and climate-related pressures.

While further studies are needed to deepen our understanding of the factors influencing mangrove dynamics in the Yangon estuary, this study provides a critical baseline, addressing key knowledge gaps and laying the groundwork for future investigations into conservation and management.

CRediT authorship contribution statement

Phyu Phway Thant: Writing – review & editing, Writing – original draft, Methodology, Investigation, Formal analysis, Data curation. **Zhijun Dai:** Writing – review & editing, Writing – original draft, Validation,

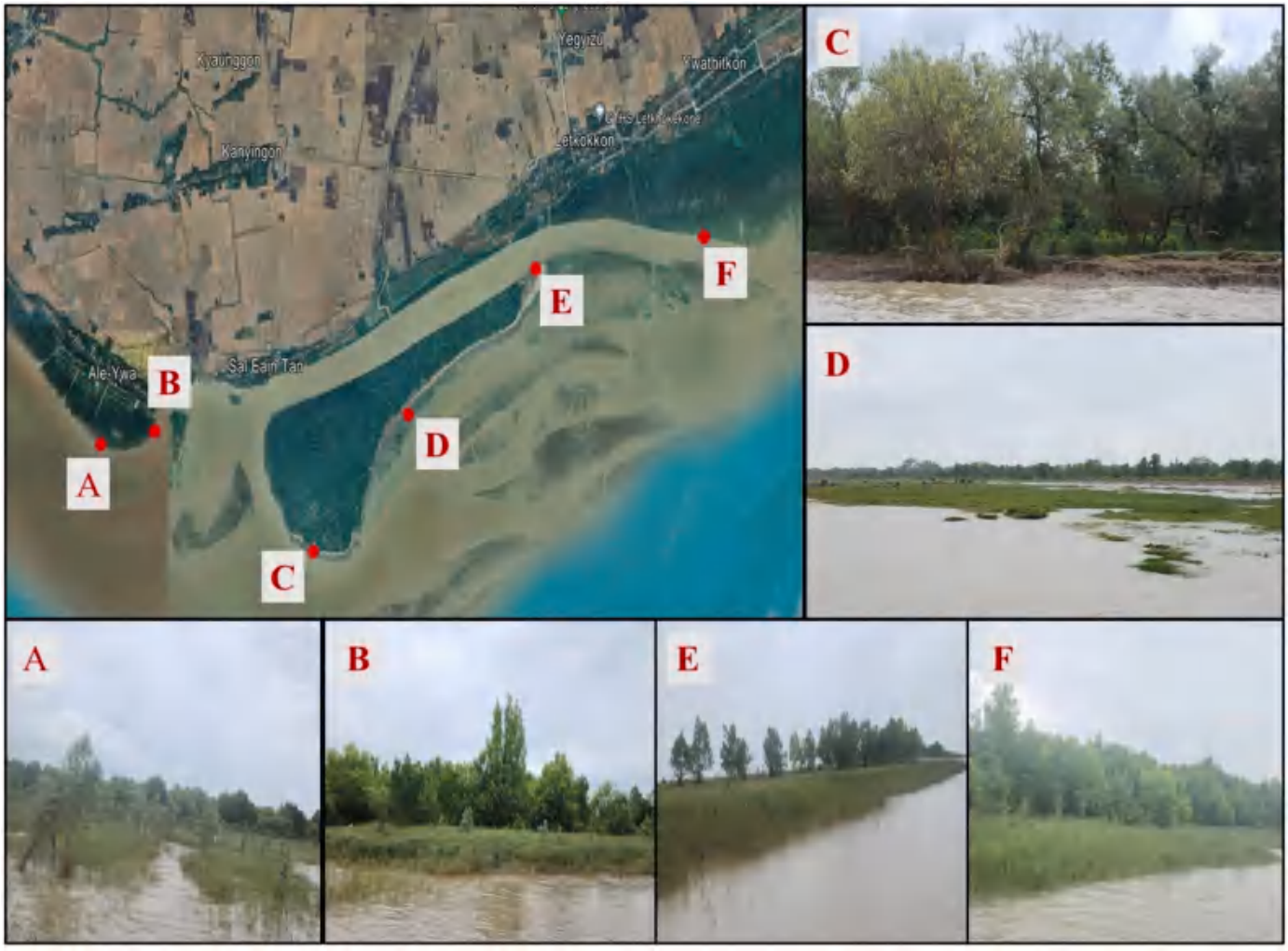

Fig. 12. Pictures from field observation in western coast. A: Aleywar with newly grown mangroves. B: Saltmarsh expansion in Aleywar area. C: Eroded south west part of MST. D: Seaward part of MST with livestock grazing. E: Eastward expansion of MST with young mangroves. F: Kanyashe mangroves accompanied by saltmarsh grasses.

Supervision, Funding acquisition, Formal analysis, Data curation, Conceptualization. **Xuefei Mei:** Writing – review & editing, Writing – original draft, Visualization, Validation, Software, Investigation. **Binh An Nguyen:** Visualization, Validation, Resources. **Cong Mai Van:** Visualization, Validation, Software, Resources. **Mee Mee Soe:** Validation, Software, Resources.

Declaration of competing interest

The authors declare that they have no known competing financial interests or personal relationships that could have appeared to influence the work reported in this paper.

Acknowledgements

This research was supported by the National Natural Science Key Foundation of China (NSFC) (41930537), Shanghai International Science and Technology Cooperation Fund Project (23230713800, 24230740100), international Joint Laboratory of Estuarine and Coastal Research, Science and Technology Commission of Shanghai Municipality (21230750600), and Ocean Decade International Cooperation Center (GHZZ37028400020240200000025). Altimetry data are provided by the NOAA Laboratory for Satellite Altimetry.

Appendix A. Supplementary data

Supplementary data to this article can be found online at https://doi.org/10.1016/j.marenvres.2025.107343.

Data availability

Data will be made available on request.

References

Ahmed, N., Thompson, S., Glaser, M., 2018. Integrated mangrove-shrimp cultivation: potential for blue carbon sequestration. AMBIO A J. Hum. Environ. 441–452.
Ai, B., Ma, C., Zhao, J., Zhang, R., 2020. The impact of rapid urban expansion on coastal mangroves: a case study in Guangdong Province China. Front. Earth Sci. 14 (1), 37–49.
Alongi, D.M., 2008. Mangrove forests: resilience, protection fromtsunamis, and responses to global climate change. Estuar. Coast Shelf Sci. 76, 1–13.
Alongi, D.M., 2009. The Energetics of Mangrove Forests. Springer Science, Dordrecht.
Alongi, D.M., 2015. The impact of climate change on mangrove forests. Curr. Clim. Chang. Rep. 1, 30–39.
Alongi, D.M., 2016. Climate regulation by capturing carbon in mangroves. In: Finlayson, C., et al. (Eds.), The Wetland Book. Springer, Dordrecht.
Anang, D.P., Asriningrum, W., 2019. Identification of mangrove forests using multispectral satellite imageries. International Journal of Remote Sensing and Earth Sciences 16 (1), 63–86.
Anthony, E., 2004. Sediment dynamics and morphological stability of estuarine mangrove swamps in Sherbro Bay, West Africa. Mar. Geol. 208, 207–224.

Anthony, E.J., Besset, M., Dussouillez, P., Goichot, M., Loisel, H., 2019. Overview of the monsoon-influenced Ayeyarwady River delta and delta shoreline mobility in response to changing fluvial sediment supply. Mar. Geol. 417, 106038.
Aung, T.T., 2022. Mangroves in Myanmar. In: Das, S.C., Pullaiah, P., Ashton, E.C. (Eds.), Mangroves: Biodiversity, Livelihoods and Conservation. Springer, Singapore, pp. 329–346.
Ball, M.C., 1988. Salinity tolerance in the mangroves Aegiceras corniculatum and Avicennia marina. I. Water use in relation to growth, carbon partitioning, and salt balance. Aust. J. Plant Physiol. 15 (3), 447–464.
Baloloy, A., Blanco, A.C., Ana, R.R.C.S., Nadaoka, K., 2020. Development and application of a new mangrove vegetation index (MVI) for rapid and accurate mangrove mapping. ISPRS J. Photogrammetry Remote Sens. 166, 95–117.
Belton, B., Filipski, M.J., Hu, C., 2017. Aquaculture in Myanmar: fish farm technology, production economics and management. Research Paper 52. Feed the Future Innovation Lab for Food Security Policy.
Besset, M., Anthony, E.J., Dussouillez, P., Goichot, M., 2017. The impact of Cyclone Nargis on the Ayeyarwady (Irrawaddy) River delta shoreline and nearshore zone (Myanmar): towards degraded delta resilience? C. R. Geosci. 349 (6–7), 238–247.
Boak, E.H., Turner, I.L., 2005. Shoreline definition and detection: a review. J. Coast Res. 21 (4), 688–703.
Brander, L.M., Wagtendonk, A.J., Hussain, S.S., McVittie, A., Verburg, P.H., Groot, R.S., Ploeg, S., 2012. Ecosystem service values for mangroves in Southeast Asia: a meta-analysis and value transfer application. Ecosyst. Serv. 1, 62–69.
Bunting, P., Rosenqvist, A., Lucas, R., Rebelo, L.M., Hilarides, L., Thomas, N., Hardy, A., Itoh, T., Shimada, M., Finlayson, C., 2018. The global mangrove watch—a new 2010 global baseline of mangrove extent. Remote Sens. 10, 1669, 2018.
Bunting, P., Rosenqvist, A., Hilarides, L., Lucas, R., Thomas, N., 2022. Global mangrove Watch: updated 2010 mangrove forest extent (v2.5). Remote Sens. 14, 1034, 2022.
Cannon, D., Kibler, K., Donnelly, M., McClenachan, G., Walters, L., Roddenberry, A., Phagan, J., 2020. Hydrodynamic habitat thresholds for mangrove vegetation on the shorelines of a microtidal estuarine lagoon. Ecol. Eng. 158, 106070.
Chandrasekar, K., Sai, M.V.R.S., Roy, P.S., Dwevedi, R., 2010. Land surface water index (LSWI) response to rainfall and NDVI using the MODIS vegetation index product. Int. J. Rem. Sens. 31, 3987–4005.
Chen, D., Lia, X., Saito, Y., Liud, J.P., Duan, Y., Liu, S., Zhang, L., 2020. Recent evolution of the Irrawaddy (Ayeyarwady) Delta and the impacts of anthropogenic activities: a review and remote sensing survey. Geomorphology 365, 107231.
Congalton, R.G., 1991. A review of assessing the accuracy of classifications of remotely sensed data. Rem. Sens. Environ. 37 (1), 35–46.
Constance, A., Haverkamp, P.J., Bunbury, N., Schaepman-Strub, G., 2021. Extent change of protected mangrove forest and its relation to wave power exposure on Aldabra Atoll. Global Ecology and Conservation 27, e01564.
Ellison, A.M., Felson, A.J., Friess, D.A., 2020. Mangrove rehabilitation and restoration as experimental adaptive management. Front. Mar. Sci. 7, 327.
Everitt, J.H., Yang, C., Summy, K.R., Judd, F.W., Davis, M.R., 2007. Evaluation of color-infrared photography and digital imagery to map black mangrove on the Texas Gulf Coast. J. Coast Res. 23 (1), 230–235.
FAO, 2003. Myanmar: Mission report on coastal aquaculture (FAO Fisheries Report No. 710). Food and Agriculture Organization of the United Nations.
FAO, 2023. The World's Mangroves 2000–2020. Rome.
Farda, N.M., 2017. Multi-temporal land use mapping of coastal wetlands area using machine learning in Google Earth Engine. IOP Conf. Ser. Earth Environ. Sci. 98, 012042.
Field, C.B., et al., 1998. Mangrove biodiversity and ecosystem function. Global Ecol. Biogeogr. 7, 3–14.
Foody, G.M., 2002. Status of land cover classification accuracy assessment. Rem. Sens. Environ. 80 (1), 185–201.
Friess, D.A., Krauss, K.W., Horstman, E.M., Balke, T., Bouma, T.J., Galli, D., Webb, E.L., 2012. Are all intertidal wetlands naturally created equal? Bottlenecks, thresholds, and knowledge gaps to mangrove and saltmarsh ecosystems. J. Ecol. 87 (2), 346–366.
Friess, D.A., Rogers, K., Lovelock, C.E., Krauss, K.W., Hamilton, S.E., Lee, S.Y., Lucas, R., Primavera, J., Rajkaran, A., Shi, S., 2019. The state of the world's mangrove forests: past, present, and future. Annu. Rev. Environ. Resour. 44, 89–115.
Furukawa, K., Wolanski, E., 1996. Sedimentation in mangrove forests. Mangroves Salt Marshes 1 (3), 183–190.
Gerona-Daga, M.E.B., Salmo III, S.G., 2022. A systematic review of mangrove restoration studies in southeast Asia: challenges and opportunities for the united nation's decade on ecosystem restoration. Front. Mar. Sci. 9, 987737.
Gilman, E.L., Ellison, J., Duke, N.C., Field, C., 2008. Threats to mangroves from climate change and adaptation options: a review. Aquat. Bot. 89 (2), 237–250.
Giri, C.P., 2016. Observation and monitoring of mangrove forests using remote sensing: opportunities and challenges. Remote Sens. 8 (10), 783.
Giri, C., Ochieng, E., Tieszen, L.L., Zhu, Z., Singh, A., Loveland, T., Masek, J., Duke, N., 2011. Status and distribution of mangrove forests of the world using Earth observation satellite data. Global Ecol. Biogeogr. 20 (1), 154–159.
Glover, H.E., Ogston, A.S., Fricke, A.T., Nittrouer, C.A., Aung, C., Naing, T., Kyu Kyu, K., Htike, H., 2021. Connecting sediment retention to distributary-channel hydrodynamics and sediment dynamics in a tide-dominated delta: the Ayeyarwady Delta, Myanmar. J. Geophys. Res.: Earth Surf. 126 (3), e2020JF005882.
Green, M.O., 2011. Dynamics of very small waves and associated sediment resuspension on an estuarine intertidal flat. Estuar. Coast. Shelf Sci. 93 (4), 449–459.
Gunasekera, R., Daniell, J.E., Pomonis, A., Macabuag, J.L.D.C., Brand, J., Jafino, B.A., De Bruijn, Cubas, D., Romero Hernandez, Oo, A.N., Cox, K.D., 2023. Extremely Severe Cyclonic Storm Mocha, May 2023, Myanmar: Global Rapid Post-Disaster Damage Estimation (GRADE) report. World Bank Group. http://documents.worldbank.org/curated/en/099010224055035000.
Hamilton, S.E., 2019. Mangroves and Aquaculture: A Five-Decade Remote Sensing Analysis of Ecuador's Estuarine Environments, vol. 33. Springer, Cham.
Hamilton, S.E., Casey, D., 2016. Creation of a high spatio-temporal resolution global database of continuous mangrove forest cover for the 21st century (CGMFC-21). Global Ecol. Biogeogr. 25, 729–738.
Harris, C.K., Wacht, J.T., Fair, M.J., Côté, J.M., 2022. ADCP observations of currents and suspended sediment in the macrotidal Gulf of Martaban, Myanmar. Front. Earth Sci. 10, 820326.
Hu, Z., Lenting, W., van der Wal, D., Bouma, T.J., 2015. Continuous monitoring bed-level dynamics on an intertidal flat: Introducing novel, stand-alone high-resolution SED-sensors. Geomorphology 245, 223–230.
Huete, A.R., et al., 2002. Overview of the radiometric and biophysical performance of the MODIS vegetation indices. Rem. Sens. Environ. 83, 195–213.
Intergovernmental Panel on Climate Change (IPCC), 2021. Climate Change 2021: the Physical Science Basis. Contribution of Working Group I to the Sixth Assessment Report of the Intergovernmental Panel on Climate Change. Cambridge University Press.
Jayanthi, M., et al., 2023. Are the Sundarbans, the world's largest mangrove region under threat? —an ecosystem-based geospatial approach to assess changes past, present, and future in relation to natural and human-induced factors. Land Degrad. Dev. 34 (1), 125–141.
JICA, 2016. Data Collection Survey Report for Improvement of Navigation Channel of Yangon Port.
Kamal, M., Jamaluddin, I., Parela, A., Farda, N.M., 2019. Comparison of Google Earth Engine (GEE)-based machine learning classifiers for mangrove mapping. In: 40th Asian Conference on Remote Sensing (ACRS 2019).
Kassakian, J.M., Friedman, M.E., 2017. Vulnerability of coastal wetlands including mangroves to sea-level rise. In: Coastal Wetlands in Changing Environments. Springer, pp. 321–351.
Kibbler, K.M., Pilato, C., Walters, L.J., Donnelly, M., Taye, J., 2022. Hydrodynamic limitations to mangrove seedling retention in subtropical estuaries. Sustainability 14 (14), 8605.
Knapp, K.R., Kruk, M.C., Levinson, D.H., Diamond, H.J., Neumann, C.J., 2010. The international best track archive for climate stewardship (IBTrACS): unifying tropical cyclone best track data. Bull. Am. Meteorol. Soc. 91 (3), 363–376.
Kuehl, S.A., Williams, J., Liu, J.P., Harris, C., Aung, D.W., Tarpley, D., Goodwyn, M., Aye, Y.Y., 2019. Sediment dispersal and accumulation off the Ayeyarwady delta: tectonic and oceanographic controls. Mar. Geol. 417, 106000.
Kumara, M.P., Jayatissa, L.P., Krauss, K.W., et al., 2010. High mangrove density enhances surface accretion, surface elevation change, and tree survival in coastal areas susceptible to sea-level rise. Oecologia 164, 545–553.
Le Minor, M., Bartzke, G., Zimmer, M., Gillis, L., Helfer, V., Huhn, K., 2019. Numerical modelling of hydraulics and sediment dynamics around mangrove seedlings: implications for mangrove establishment and reforestation. Estuar. Coast Shelf Sci. 217, 81–95.
Leal, M., Spalding, M.D., 2022. The State of the World's Mangroves 2022, Global Mangrove Alliance.
Leal, M., Spalding, M.D. (Eds.), 2024. The State of the World's Mangroves 2024. Global Mangrove Alliance.
Lewis, R.R., 2005. Ecological engineering for successful management and restoration of mangrove forests. Ecol. Eng. 24 (4), 403–418. https://doi.org/10.1016/j.ecoleng.2004.10.003.
Lewis, R.A., 2006. Five steps to successful ecological restoration of mangroves (The Manual). Mangrove Action Project/Yayasan Akar Rumput Laut, Yogyakarta.
Li, X., Liu, J.P., Saito, Y., Nguyen, V.L., 2017. Recent evolution of the Mekong Delta and the impacts of dams. Earth Sci. Rev. 175, 1–17.
Li, W., El-Askary, H., Qurban, M.A., Li, J., Manikandan, K., Piechota, T., 2019. Using a multi-indices approach to quantify mangrove changes over the Western Arabian Gulf along the Saudi Arabia coast. Ecol. Indic. 102, 734–745.
Liu, J.P., Kuehl, S.A., Pierce, A.C., Williams, J., Blair, N.E., Harris, C., Aung, D.W., Aye, Y. Y., 2020. Fate of Ayeyarwady and thanlwin rivers sediments in the Andaman Sea and Bay of bengal. Mar. Geol. 423, 106137.
Long, C., Dai, Z., Zhou, X., Mei, X., Van, C.M., 2021. Mapping mangrove forests in the red river delta, Vietnam. For. Ecol. Manag. 483, 118910.
Long, C., et al., 2022. Dynamic changes in mangroves of the largest delta in northern Beibu Gulf, China: reasons and causes. For. Ecol. Manag. 504, 119855.
Lovelock, C.E., Cahoon, D.R., Friess, D.A., Guntenspergen, G.R., Krauss, K.W., Reef, R., Rogers, K., Saunders, M.L., Sidik, F., Swales, A., Saintilan, N., Thuyen, L.X., Triet, T., 2015. The vulnerability of Indo-Pacific mangrove forests to sea-level rise. Nature 526 (7574), 559–563.
Lovelock, C.E., Feller, I.C., Reef, R., Hickey, S., Ball, M.C., 2017. Mangrove dieback during fluctuating sea levels. Sci. Rep. 7 (1), 1680.
Lovelock, C.E., Reef, R., Masqué, P., 2021. Vulnerability of an arid zone coastal wetland landscape to sea level rise and intense storms. Limnol. Oceanogr. 1–14.
Lwin, A., Khaing, M.M., 2012. Yangon River geomorphology identification and its environmental impacts analysis by optical and radar sensing techniques. In: International Archives of the Photogrammetry, Remote Sensing and Spatial Information Sciences, vol. XXXIX-B8, pp. 175–179.
Marini, Y., Manoppo, A., Anggraini, N., 2015. Teknik penentuan komposit warna RGB untuk identifikasi mangrove di Pulau Subi Kecil menggunakan data Landsat 8 in Buku Buka Rampai Mangrove.
Mondal, P., Liu, X., Fatoyinbo, T.E., Lagomasino, D., 2019. Evaluating combinations of Sentinel-2 data and machine-learning algorithms for mangrove mapping in West Africa. Remote Sens. 11, 2928.

Myanmar National Adaptation Programme of Action (NAPA), 2012.
Nelson, B.W., 2000. Sediment dynamics in rangoon river, Myanmar. Sci. Total Environ. 266, 15–21.
Osland, M.J., Feher, L.C., Day, R.H., Stagg, C.L., 2017. Climatic controls on the global distribution, abundance, and species richness of mangrove forests. Ecol. Monogr. 87 (3), 341–359.
Park, S., 2004. Aspects of Mangrove Distribution and Abundance in Tauranga Harbour, vol. 16. Environment Bay of Plenty Environmental Publication, p. 40.
Paul, A.K., Kamila, A., Ray, R., 2018. Natural threats and impacts to mangroves within the coastal fringing forests of India. In: Faridah-Hanum, I., Latiff, A., Hakeem, K.R., Ozturk, M. (Eds.), Threats to Mangrove Forests: Hazards, Vulnerability. and Management, pp. 129–150.
Peterson, J.M., Bell, S.S., 2015. Saltmarsh boundary modulates dispersal of mangrove propagules: implications for mangrove migration with sea-level rise. PLoS One 10 (3), e0119128.
Pilato, C., 2019. Hydrodynamic Limitations and the Effects of Living Shoreline Stabilization on Mangrove Recruitment along Florida Coastlines (Master's Thesis). University of Central Florida.
Polidoro, B.A., Carpenter, K.E., Collins, L., Duke, N.C., Ellison, A.M., Ellison, J.C., Farnsworth, E.J., Fernando, E.S., Kathiresan, K., Koedam, N.E., Livingstone, S.R., Miyagi, T., Moore, G.E., Nam, V.N., Ong, J.E., Primavera, J.H., Salmo, S.G., Sanciangco, J.C., Sukardjo, S., et al., 2010. The loss of species: mangrove extinction risk and geographic areas of global concern. PLoS One 5 (4), e10095.
Ramaswamy, V., Rao, P.S., Rao, K.H., Thwin, S., Srinivasa Rao, N., Raiker, V., 2004. Tidal influence on suspended sediment distribution and dispersal in the northern Andaman Sea and Gulf of Martaban. Mar. Geol. 208 (1–4), 33–42.
Richards, D.R., Friess, D.A., 2016. Rates and drivers of mangrove deforestation in southeast Asia, 2000-2012. Proc. Natl. Acad. Sci. U. S. A. 113, 344–349.
Rouse, J.W., Haas, R.H., Schell, J.A., Deering, D.W., 1974. Monitoring vegetation systems in the great plains with ERTS. NASA Spec. Publ. 351 (1), 309.
Sakho, I., Mesnage, V., Deloffre, J., Lafite, R., Niang, I., Faye, G., 2011. The influence of natural and anthropogenic factors on mangrove dynamics over 60 years: the Somone estuary, Senegal. Estuarine. Coastal and Shelf Science 94, 93–101.
Sawant, S., Bonala, P., Joshi, A., et al., 2024. Integration of machine learning and remote sensing for assessing the change detection of mangrove forests along the Mumbai coast. J. Earth Syst. Sci. 133 (1), 186.
Shi, T., Liu, J., Hu, Z., Liu, H., Wang, J., Wu, G., 2016. New spectral metrics for mangrove forest identification. Remote Sensing Letters 7 (9), 885–894.
Shimozono, T., Tajima, Y., Akamatsu, S., Matsuba, Y., Kawasaki, A., 2019. Large-scale channel migration in the Sittang River estuary. Sci. Rep. 9. Article 9862.
Sindhu, B., Unnikrishnan, A.S., 2013. Characteristics of tides in the Bay of bengal. Mar. Geod. 36 (4), 377–407.
Sir Alexander Gibb and Partners, 1974. Rangoon Sea access channel & associated Port improvement study. United nations development programme. International Bank for Reconstruction and Development, Burma Port Corporation (Only hardcopy available).
Smoak, J.M., Breithaupt, J.L., Smith III, T.J., Sanders, C.J., 2013. Sediment accretion and organic carbon burial relative to sea-level rise and storm events in two mangrove forests in Everglades National Park. Catena 104, 58–66.
Souza Filho, P.W.M., Martins, E. do S.F., Costa, F.R., 2006. Using mangroves as a geological indicator of coastal changes in the Bragança macrotidal flat, Brazilian Amazon: a remote sensing data approach. Ocean Coast Manag. 49 (8–9), 462–475.
Spalding, M., 2010. World Atlas of Mangroves. Routledge, London.
Sunkur, R., Kantamaneni, K., Bokhoree, C., Ravan, S., 2023. Mangroves' role in supporting ecosystem-based techniques to reduce disaster risk and adapt to climate change: A review. J. Sea Res. 196, 102449.
Swales, A., Reeve, G., Cahoon, D.R., Lovelock, C.E., 2019. Landscape evolution of a fluvial sediment-rich Avicennia marina mangrove forest: insights from seasonal and inter-annual surface-elevation dynamics. Ecosystems 1–24.
Tarpley, J.D., Schneider, S.R., Money, R.L., 1984. Global vegetation indices from the NOAA-7 meteorological satellite. J. Appl. Meteorol. Climatol. 23 (3), 491–494.
Thakur, S., Mondal, I., Ghosh, P.B., Das, P., De, T.K., 2019. A review of the application of multispectral remote sensing in the study of mangrove ecosystems with special emphasis on image processing techniques. Journal of Spatial Information Research 28 (3), 39–51.
2001 Tide Tables 2002: Central Pacific Ocean and Indian Ocean, 2001. International Marine.
Tinh, P.H., et al., 2022. Distribution and drivers of Vietnam mangrove deforestation from 1995 to 2019. Mitig. Adapt. Strategies Glob. Change 27 (4), 29.
Twilley, R.R., Day, J.W., 2013. Chapter 7. Mangrove wetlands. In: Day, J.W., Crump, B. C., Kemp, W.M., Yanez-Arancibia, A. (Eds.), Estuarine Ecology. Wiley-Blackwell, Hoboken, pp. 165–202.
Uncles, R.J., Stephens, J.A., 2000. Observations of currents, salinity, turbidity and intertidal mudflat characteristics in the Tavy Estuary, UK. Cont. Shelf Res. 20 (12–13), 1461–1478.
United Nations Environment Programme, 2023. Decades of Mangrove Forest Change: what Does it Mean for Nature, People and the Climate? UNEP, Nairobi.
Veettil, B.K., Pereira, S.F.R., Quang, N.X., 2018. Rapidly diminishing mangrove forests in Myanmar (Burma): a review. Hydrobiologia 822 (1), 19–35.
Veettil, B.K., Quang, N.X., Trang, N.T.T., 2019. Changes in mangrove vegetation, aquaculture, and paddy cultivation in the Mekong Delta: a study from Ben Tre province, southern Vietnam. Estuarine. Coastal and Shelf Science 226. Article 106273.
Wang, L., Sousa, W.P., Gong, P., Biging, G.S., 2004. Comparison of IKONOS and QuickBird images for mapping mangrove species on the Caribbean coast of Panama. Rem. Sens. Environ. 91 (3–4), 432–440.
Ward, R.D., Drude de Lacerda, L., 2021. Chapter 10: responses of mangrove ecosystems to sea level change. In: Dynamic Sedimentary Environments of Mangrove Coasts, pp. 235–253.
Ward, R., Friess, D., Day, R., Mackenzie, R., 2016. Impacts of climate change on global mangrove ecosystems: a regional comparison. EHS 2 (4), 1–25.
Whitty, T.S., Maw, T.Z., 2023. State of the Gulf of Mottama Report. Gulf of Mottama Project (GoMP).
Woodroffe, C.D., Grindrod, J., 1991. Mangrove biogeography: the role of Quaternary environmental and sea-level change. J. Biogeogr. 18 (5), 479–492.
Worthington, T.A., Ermgassen, P., Friess, D.A., Krauss, K.W., Lovelock, C.E., Thorley, J., Tingey, J., Woodroffe, C.D., Bunting, P., Cormier, N., Lagomasino, D., Lucas, R., Murray, N., Sutherland, W.J., Spalding, M., 2020. A global biophysical typology of mangroves and its relevance for ecosystem structure and deforestation. Sci. Rep. 10 (1), 14652.
Wyrtki, K., 1961. Physical Oceanography of the Southeast Asian Waters. University of California, California.
Xiao, X., et al., 2004. Modeling gross primary production of temperate deciduous broadleaf forest using satellite images and climate data. Rem. Sens. Environ. 91, 256–270.
Xiong, Y., Dai, Z., Long, C., Liang, X., Lou, Y., Mei, X., Nguyen, B.A., Cheng, J., 2024. Machine Learning-Based examination of recent mangrove forest changes in the western Irrawaddy River Delta, Southeast Asia. Catena 234, 107601.
Xu, H., 2006. Modification of normalized difference water index (NDWI) to enhance open water features in remotely sensed imagery. Int. J. Rem. Sens. 27 (14), 3025–3033.
Zhang, Z., Ahmed, M.R., Zhang, Q., Li, Y., Li, Y., 2023. Monitoring of 35-year mangrove wetland change dynamics and agents in the Sundarbans using temporal consistency checking. Remote Sens. 15 (3), 625.
Zhou, Y., Dai, Z., Liang, X., Cheng, J., 2024. Machine learning-based monitoring of mangrove ecosystem dynamics in the Indus Delta. For. Ecol. Manag., 122231